

CHAPTER VI
AN IN SITU INFRARED STUDY OF CO HYDROGENATION AND
ETHYLENE HYDROFORMYLATION ON Ru/SiO₂ AND SULFIDED Ru/SiO₂

6.1 Introduction

Syngas (CO/H₂) and related reactions constitute important pathways for the conversion of coal to chemical feedstocks and liquid fuel [1,2]. One of the most important syngas related reactions is the hydroformylation of olefins that represents the largest volume use of syngas in homogeneously catalyzed reactions [47,48]. Extensive mechanistic studies have shown that the homogeneous hydroformylation reaction proceeds via (i) the insertion of CO into alkyl-metal complexes leading to the formation of acyl-complex intermediates and then followed by (ii) the hydrogenolysis to give aldehydes [45-49]. The hydroformylation mechanism has often been used as a model to explain the formation of C₂₊ aldehydes and alcohols in the Fischer-Tropsch (F-T) synthesis (heterogeneous CO hydrogenation) [39,54,55]. Probing the mechanism of CO hydrogenation by olefin additions has shown that the reaction of added olefins with syngas on the supported Ru and Rh metals leads to the formation of aldehydes [55,58,74]. The reaction for the formation of aldehydes on the supported Ru and Rh catalysts has been considered as the heterogeneous

hydroformylation that resembles the homogeneous hydroformylation catalyzed by metal complexes [39,57].

The hydroformylation reaction that is homogeneously catalyzed reaction was first discovered on the heterogeneous F-T cobalt (Co) catalyst [47]. It was later recognized that the Co carbonyls produced from the heterogeneous Co metal during the reaction were responsible for the reaction [47-49]. The interesting development of the hydroformylation mechanism on the Co catalyst has led us to raise an important question concerning the nature of hydroformylation on the Ru/SiO₂ catalyst that is one of the most active F-T catalysts [8,23,70]. Is the hydroformylation reaction on the supported Ru catalyst a truly heterogeneously catalyzed reaction ?

Sulfur is known to be a severe poison to the heterogeneous metal catalysts that catalyze CO hydrogenation, olefin hydrogenation, paraffin hydrogenolysis, and hydrocarbon related reactions [96-98]. The poisoning effect of sulfur compounds on the metal surface has been attributed to the blockage of active sites as well as the modification of surface states of the catalyst by adsorbed sulfur. Interestingly, several recent studies have shown that sulfur compounds such as H₂S slightly enhanced ethylene hydroformylation over Rh/SiO₂ and Ni/SiO₂ catalysts [55,112] but inhibited the reaction on Ru/SiO₂ [74]. The failure of sulfur to poison the hydroformylation reaction on the Ni and Rh catalysts has been ascribed to the inability of adsorbed sulfur to deactivate the single atom site that is responsible for the reaction. However, the mechanism for sulfur poisoning of Ru catalysts in the hydroformylation reaction is still not understood. Because syngas, produced from coal, usually contaminates with a significant amount of

sulfur compounds such as H_2S , developing a better understanding of the role of sulfur in syngas reaction and hydroformylation is of great technological importance. 88

The objective of this study was to investigate the nature of ethylene hydroformylation over Ru/SiO_2 and the role of sulfur in the reaction. An in situ infrared spectroscopic (IR) technique was employed to study CO adsorption, CO hydrogenation, and ethylene hydroformylation on Ru/SiO_2 and sulfided Ru/SiO_2 catalysts. Results of CO adsorption and CO hydrogenation were compared with those of hydroformylation to clarify the IR bands of various adsorbed species. The dynamic behavior of all adsorbed species during the hydroformylation was examined by a transient experiment in which a steady-state $CO/H_2/C_2H_4$ flow was switched to a steady-state CO/H_2 flow. The reactivity of the adsorbed species with H_2 was studied by temperature-programmed reaction (TPR) with H_2 . Due to the presence of the residual chlorine on the Ru/SiO_2 catalyst used in this study, the effect of chlorine on the vibrational frequency of adsorbed CO was also examined.

6.2 Experimental

6.2.1 Catalyst Preparation and Characterization

The 3 wt% Ru/SiO_2 catalyst was prepared by impregnation of SiO_2 using $RuCl_3 \cdot 3H_2O$. The preparation procedure is described in Chapter III. Sulfidation was conducted by exposure of Ru/SiO_2 to flowing H_2S flow (1000 ppm H_2S in H_2) at 513 K for 1 hr. The bulk ratio of sulfur to ruthenium was determined by energy-dispersive spectroscopy (EDS). Ru crystallite sizes before and after sulfidation was determined to be 80 Å by X-ray diffraction (XRD) line-broadening technique. No

significant difference in XRD spectra for the sulfided and unsulfided Ru indicates that sulfidation at 513 K could reach only to the surface of the particle rather than the entire particle of Ru. Hydrogen uptake for the Ru/SiO₂ and the sulfided Ru/SiO₂ (S-Ru/SiO₂) was measured by hydrogen temperature-programmed desorption. The residual chlorine in the reduced Ru/SiO₂ was determined by Galbraith Lab, Inc. The catalyst was pressed into a self-supporting disk with 20 mg.

6.2.2 Experimental Procedure

CO hydrogenation and ethylene hydroformylation were studied in steady-state flow conditions of 513 K and 10-30 atm in the IR cell which can be considered as a differential reactor. Gas phase CO bands were eliminated by subtracting the absorbance of gas phase CO with a SiO₂ disk in the cell from the spectra of gaseous reactants and products as well as adsorbed species on the Ru/SiO₂ and S-Ru/SiO₂ catalysts. Subsequent to recording each IR spectrum, the effluent of the IR cell was sampled and analyzed by an on-line gas chromatography.

The transient infrared study was conducted by switching a steady-state C₂H₄/CO/H₂ flow to a steady-state CO/H₂ flow and maintaining at constant pressure. The change in the IR intensity of adsorbed species during the switch was closely monitored by the infrared spectrometer.

Following steady-state ethylene hydroformylation, reactor temperatures and pressures were decreased to 303 K and 1 atm. The temperature-programmed reaction (TPR) was then carried out by introducing a flow of H₂ to the IR cell at 10 cm³/min and heating the

reactor at a rate of 5 K/min to 513 K. IR spectra were taken during ⁹⁰ the entire course of the TPR study.

6.3 Results and Discussion

6.3.1 CO Adsorption

Figure 6.1 shows the infrared spectra of CO adsorption on the Ru/SiO₂ and the S-Ru/SiO₂ catalysts at 513 K. It should be noted that the Ru/SiO₂ used in this study contains 0.5 wt% residual chlorine. Two bands were observed for CO adsorption on the Ru/SiO₂ catalyst at 10 atm: a linear CO band at 2040 cm⁻¹ and a weak bridge CO band at about 1787 cm⁻¹. The observed wavenumbers of adsorbed CO are in good agreement with those reported for Ru/SiO₂ [23,35,128]. Decreasing the pressure of CO from 10 to 1 atm caused a slightly downward shift of the linear CO wavenumber. Admission of H₂ to the reactor at 513 K resulted in a decrease in the intensity of the linear CO and in a downward shift of its wavenumber. Such a downward shift can be attributed to the reduction in dipole-dipole coupling [118] as a result of the removal of the adsorbed CO by reaction with hydrogen.

The influence of sulfur on the infrared spectra for adsorbed CO is also shown in Figure 6.1. Sulfidation of the catalyst resulted in (i) a reduction in the intensity of the linear CO band, (ii) a downward shift of the linear CO wavenumber, and (iii) a suppression of the weak bridge CO band. Adsorbed sulfur appeared to disrupt the adjacent pairs of Ru metal atoms, and therefore suppressing bridge CO sites. The inhibition of CO adsorption in the bridge form brought about by adsorbed sulfur has also been reported for Ni and Rh [96,97,112]. The results of (i) and (ii) may be due to a lower concentration of adsorbed CO on the surface of sulfided Ru (S-Ru) rather than a ligand effect of

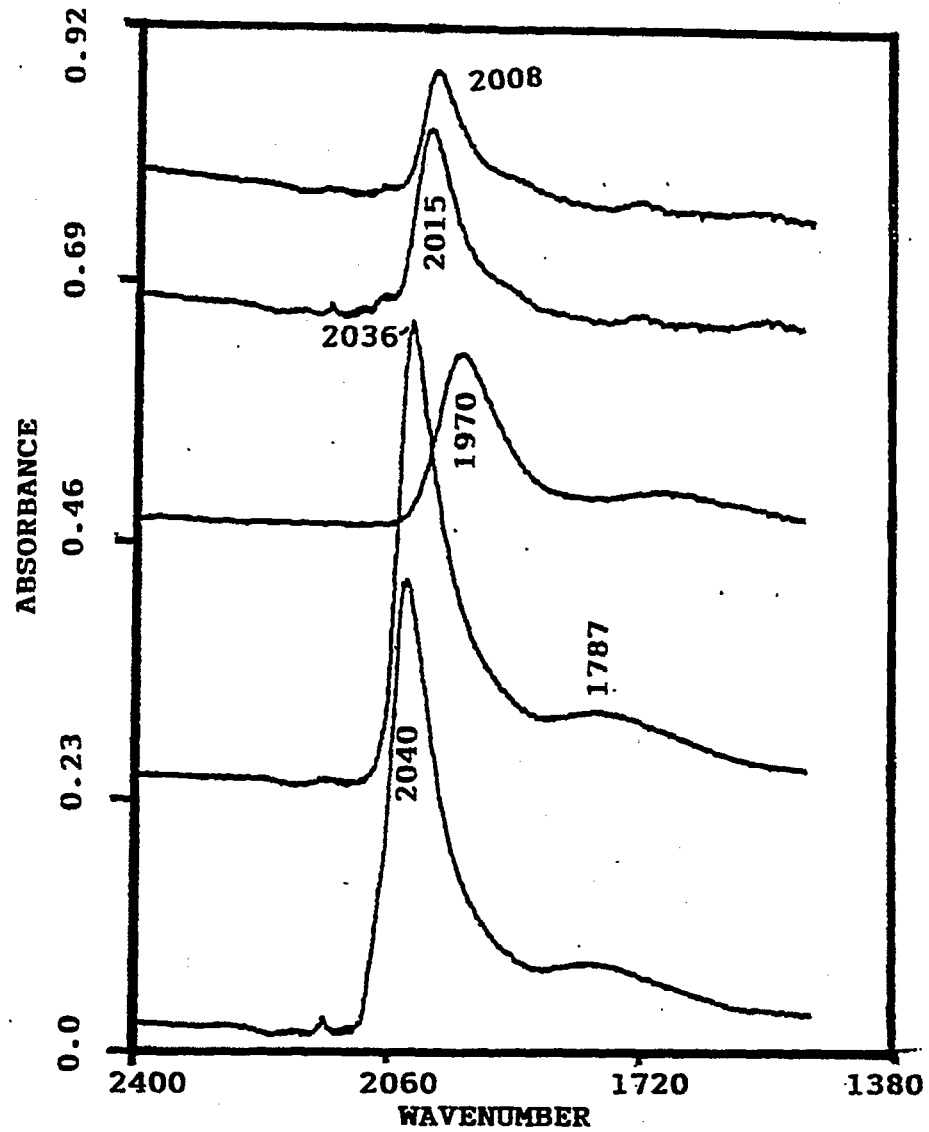


Figure 6.1 Infrared Spectra of CO Adsorption at 513 K: (a) on Ru/SiO₂ at 10 atm for 20 min, (b) at 1 atm for 20 min, (c) after reduction in flowing H₂ at a rate of 5 cm³/min at 1 atm for 20 min, (d) on S-Ru/SiO₂ at 10 atm for 20 min, (e) at 1 atm for 20 min.

adsorbed sulfur [98]. The effect of sulfur on the CO adsorbed on Ru ⁹² has been found to differ from the effect on Ni and Pt [97,108]. An upward shift of the wavenumber for the linear CO has been observed on the sulfided Ni and Rh [97,112]. The sulfided Ni and Rh catalysts showed a lower bonding energy for the CO than the unsulfided catalysts [97].

The decrease in CO pressures from 10 to 1 atm resulted in a slight modification of the intensity and wavenumber of linear CO on the Ru/SiO₂, but a marked decrease in the intensity and a downward shift of the wavenumber for linear CO on the S-Ru/SiO₂. The greater dependence of the intensity of the linear CO on the CO pressure reflects a smaller equilibrium constant for the adsorption of CO on the S-Ru/SiO₂.

6.3.2 CO Hydrogenation on Ru/SiO₂

The effect of reaction pressure on the infrared spectra for Ru/SiO₂ and S-Ru/SiO₂ are shown in Figure 6.2. Table 6.1 presents results of the rates of product formation from CO hydrogenation corresponding to IR spectra taken under steady-state conditions. The TOFs for CO conversion on the Ru/SiO₂ catalyst are lower than those reported in the literature [34]. This may be due to the use of higher ratio of CO/H₂. The major bands observed for the CO hydrogenation at 513 K and 1 atm were the linear CO band at 2003 cm⁻¹ and bands corresponding to hydrocarbon species in the region of 2860-2970 cm⁻¹ and 1461 cm⁻¹ [115]. Methane was identified to be the major product while no oxygenates were observed under this reaction condition.

As reaction pressure increased from 1 to 10 atm, the linear CO shifted from 2003 cm⁻¹ to 2020 cm⁻¹ and its intensity increased; the intensity of hydrocarbon bands and the rate of hydrocarbon formation

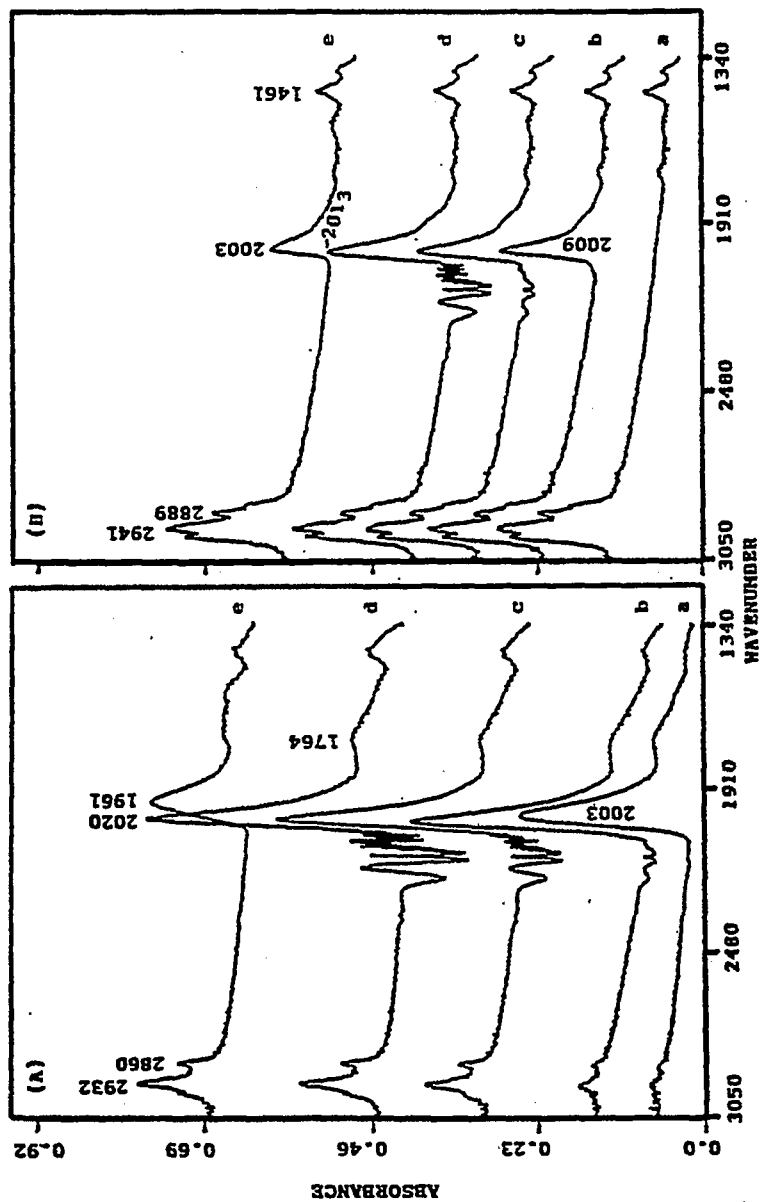


Figure 6.2 Infrared Spectra of CO/H₂ Reaction at 513 K: (A)- (a) on Ru/SiO₂ at 1 atm, (b) at 10 atm, (c) at 20 atm, (d) at 30 atm, (e) reduction in flowing H₂ at a rate of 5 cm³/min at 1 atm for 20 min; (B)- (a) background: reduction in flowing H₂ at a rate of 5 cm³/min for 10 hr after the CO/H₂/C₂H₄ reaction, (b) CO/H₂ reaction on S-Ru/SiO₂ at 1 atm, (c) at 10 atm, (d) at 30 atm, (e) reduction in flowing H₂ at a rate of 5 cm³/min at 1 atm of 20 min.

Table 6.1 CO Hydrogenation over Ru/SiO₂ and Sulfided Ru/SiO₂

Pressure (atm)	1	1	10	10	20	30
Ru/SiO ₂ Catalyst 10 ⁻³ × TOF (sec ⁻¹)	0.13	-	0.76	-	0.73	1.2
Product Formation (gmol/kg-hr)						
CH ₄	0.011	0.025 ^c	0.041	0.132 ^c	0.037	0.041
C ₂ H ₄	0.00	0.002	0.005	0.006	0.004	0.004
C ₂ H ₆	0.001	0.001	0.0007	0.003	0.0006	0.0006
C ₃ HC	0.0005	0.004	0.006	0.038	0.005	0.005
CH ₃ CHO	0.00	0.00	0.005	0.00	0.008	0.031
CH ₃ CHO/CH ₄ ^a	0.00	0.00	0.122	0.00	0.216	0.756
CH ₃ CHO/C ₂ H ₄	0.00	0.00	0.427	0.00	0.833	3.23
S-Ru/SiO ₂ Catalyst ^b Product Formation (gmol/kg-hr)						
CH ₄	0.010	-	0.023	-	0.028	-

Temperature: 513 K; CO:H₂ = 1:1

The residual chlorine content of Ru/SiO₂: 0.5 wt%

The product with formation rate smaller than 1E-2 indicates a trace produce

a: CH₃CHO/CH₄ is the ratio of the CH₃CHO formation rate to the CH₄ formation rate.

b: The ratio of S to Ru for S-Ru/SiO₂ is determined to be 0.12 by EDS.

c: The rate of product formation on the washed Ru/SiO₂ catalyst that contains 449 ppm residual chlorine.

also increased (shown in Table 6.1). Further increases in reaction 95
pressure increased the intensity of hydrocarbon bands, but did not
affect the intensity and wavenumber of the linear CO at pressures above
10 atm. The stability of these adsorbed CO and hydrocarbons were
examined by treating the catalyst in flowing H₂ (10 cm³/min) at 513 K
and 1 atm. As shown in Figure 6.2(A)-e, a decrease in the intensity of
the linear CO band was accompanied by a downward shift of the band. In
contrast, the intensity of the hydrocarbon bands were not affected by
flowing hydrogen, indicating that these hydrocarbons may be inert
spectator species [137] and adsorbed on the silica support. Unreactive
surface hydrocarbons have also been observed on the CO hydrogenation on
alumina-supported Ru catalysts. These hydrocarbon species were formed
on the Ru metal surface and then migrated onto the alumina support.
[34,127].

Table 6.1 shows that the rate of acetaldehyde formation
increased with reaction pressure. It has been suggested that C₂
oxygenates such as acetaldehyde and ethanol are formed via the
insertion of CO into CH_x which is produced from carbon monoxide
dissociation followed by hydrogenation [20,39,57-60].

Because the formation of C₂ oxygenates, methane and C₂
hydrocarbons involves a common intermediate, CH_x, a higher ratio of
CH₃CHO/CH₄ represents a higher CO insertion selectivity. The increase
in the ratio of CH₃CHO/CH₄ and CH₃CHO/C₂.HC with increasing pressures
(see Table 6.1) indicates that CO insertion competed favorably with
hydrogenation and chain growth at higher reaction pressures. However,
the intensity and the wavenumber of the linear CO band are relatively
insensitive to the overall reaction pressure in the range from 10 to 30

atm. No obvious relation between IR spectra of the adsorbed CO and ⁹⁶ the activity for CO insertion can be discerned.

Comparison of IR spectra of adsorbed CO in the CO hydrogenation reaction (Figure 6.2) with those in the CO adsorption study on Ru/SiO₂ (Figure 6.1) reveals that the linear CO in the CO/H₂ atmosphere exhibited a lower wavenumber and a lower absorbance compared to that observed in the pure CO atmosphere. The downward shift accompanied by the decreases in the absorbance for the adsorbed CO may be attributed to the decrease in dipole-dipole interactions as a result of dilution by adsorbed hydrogen [118] rather than the ligand effect of adsorbed hydrogen [37].

6.3.3 CO Hydrogenation on Sulfided Ru/SiO₂

As shown in Table 6.1, the addition of sulfur inhibited the formation of both C₂₊ hydrocarbons and oxygenates. Methane was the only product observed on the sulfided catalyst. Increasing the pressure from 1 to 30 atm enhanced the rate of the methane formation by a factor of 2.8. Comparison of the rate of methane formation on Ru/SiO₂ and S-Ru/SiO₂ shows that sulfur slightly inhibited the rate of methane formation at 1 atm. A more pronounced suppression of the rate of methane formation by sulfur was observed at higher pressures. Sulfur appears to have a small effect on the methane formation but a great inhibition effect on the production of C₂₊ hydrocarbons and oxygenates. Energy-dispersive spectroscopic studies of the S-Ru/SiO₂ showed that the bulk ratio of S to Ru was 0.12. Hydrogen TPD studies showed that sulfidation led to the loss of hydrogen chemisorption capacity [74]. Several single crystal studies have shown that a sulfur coverage of 0.33 on the Ru(111) surface could result in the complete

suppression of hydrogen chemisorption [107]; a similar sulfur coverage on the Ru(0001) decreased the methanation activity by a factor of 10 [98]. Due to the lack of information on the sulfur coverage for the S-Ru/SiO₂, a meaningful comparison between the reaction on the sulfided Ru/SiO₂ and the Ru single crystal can not be made.

The infrared spectra corresponding to the rate data shown in Table 6.1 are presented in Figure 6.2(B). The spectrum 6.2(B)-a is the background spectrum recorded for the used Ru/SiO₂ that had been exposed to CO/H₂/C₂H₄ reactant mixture and then followed by reduction in flowing hydrogen for 10 hr and sulfidation for 1 hr at 513 K. Some hydrocarbon species on the catalyst were observed by infrared spectroscopy. It is important to note that those hydrocarbon bands in the IR background have no effect on the performance of the sulfided Ru. Sulfidation of the used Ru/SiO₂ catalysts and the fresh Ru/SiO₂ resulted in the same activity and selectivity. The major spectral feature for CO hydrogenation on the sulfided catalyst is the linear CO at 2009-2013 cm⁻¹. The hydrocarbon bands at 2860-2960 cm⁻¹ exhibiting the same intensity at various conditions appear to be spectator species.

Comparison of the IR spectra for Ru/SiO₂ and S-Ru/SiO₂ (see Figure 6.2) shows the major effect of adsorbed sulfur on the adsorbed CO during CO hydrogenation is to decrease its intensity. Flowing hydrogen over the catalysts at 513 K (see spectra 6.2(A)-e and 6.2(B)-e) caused a downward shift of the linearly adsorbed CO by 59 cm⁻¹ on Ru/SiO₂ and by 10 cm⁻¹ on S-Ru/SiO₂ and a more decrease in the CO intensity for Ru/SiO₂ than for S-Ru/SiO₂. Such a less shift and decrease of the adsorbed CO on the S-Ru/SiO₂ catalyst may be due to the

fact that adsorbed sulfur inhibits hydrogen chemisorption [96-98]. 98

As a result, less adsorbed hydrogen was available to react with CO and to remove CO from the surface of sulfided Ru/SiO₂ catalyst. The observed inhibition effects of sulfur on CO adsorption and CO hydrogenation in this study are, in some respects, consistent with those reported in the literature [96-98]. Adsorbed sulfur has been found to block the bridge CO sites, weaken the metal-CO bond, and inhibit CO hydrogenation.

6.3.4 Ethylene Hydroformylation on Ru/SiO₂

Table 6.2 shows the influence of reaction pressure on the rate of product formation for CO/H₂/C₂H₄ reaction (hydroformylation) over Ru/SiO₂. The formation of CH₄, C₃+ hydrocarbons, C₂ oxygenates, ethane, and propionaldehyde indicates that CO hydrogenation, ethylene hydrogenation, and ethylene hydroformylation take place at the same time. Higher rates of C₄ hydrocarbon formation than C₃ hydrocarbon formation suggest that dimerization of ethylene occurred to a significant extent. Although the rate of formation of all the products increased with increasing pressure, there was significant variation in the pressure effect on the rate of product formation. As reaction pressure increased from 1 to 30 atm, the rate of methane formation increased by a factor of 2; the rate of ethane formation increased by a factor of 7.7; and the rate of propionaldehyde formation increased by a factor of 65. The extent of pressure effect on the rate of product formation decreased in the order: C₂H₅CHO > C₂H₄ > CH₄, suggesting that CO insertion is highly favorable at high pressures.

Figure 6.3 shows the infrared spectra taken under steady-state CO/H₂/C₂H₄ reaction conditions corresponding to the reaction results

Table 6.2 CO/H₂/C₂H₄ Reaction over Ru/SiO₂

Product Formation (gmol/kg-hr)	Pressure (atm)				
	1	1	10	10	30
CH ₄	0.023	0.018 ^a	0.037	0.078 ^a	0.042
C ₂ H ₆	0.214	0.469	1.23	8.81	1.19
C ₃ HC	0.004	0.015	0.013	0.091	0.016
C ₄ HC	0.011	0.089	0.034	0.401	0.034
C ₅ HC	0.00	0.014	0.00	0.099	0.00
CH ₃ CHO	0.00	0.00	0.00	0.008	0.006
C ₂ H ₅ CHO	0.010	0.121	0.290	3.34	0.461
C ₂ H ₅ CHO/C ₂ H ₆	0.047	0.257	0.236	0.379	0.387
					0.390

Temperature: 513 K, CO:H₂:C₂H₄ = 1:1:1
 The chlorine content of Ru/SiO₂: 0.5 wt%
 The product with formation rate smaller than 1E-2 indicates a trace produce

a: The rate of product formation on the washed Ru/SiO₂ catalyst that contains 449 ppm chlorine.

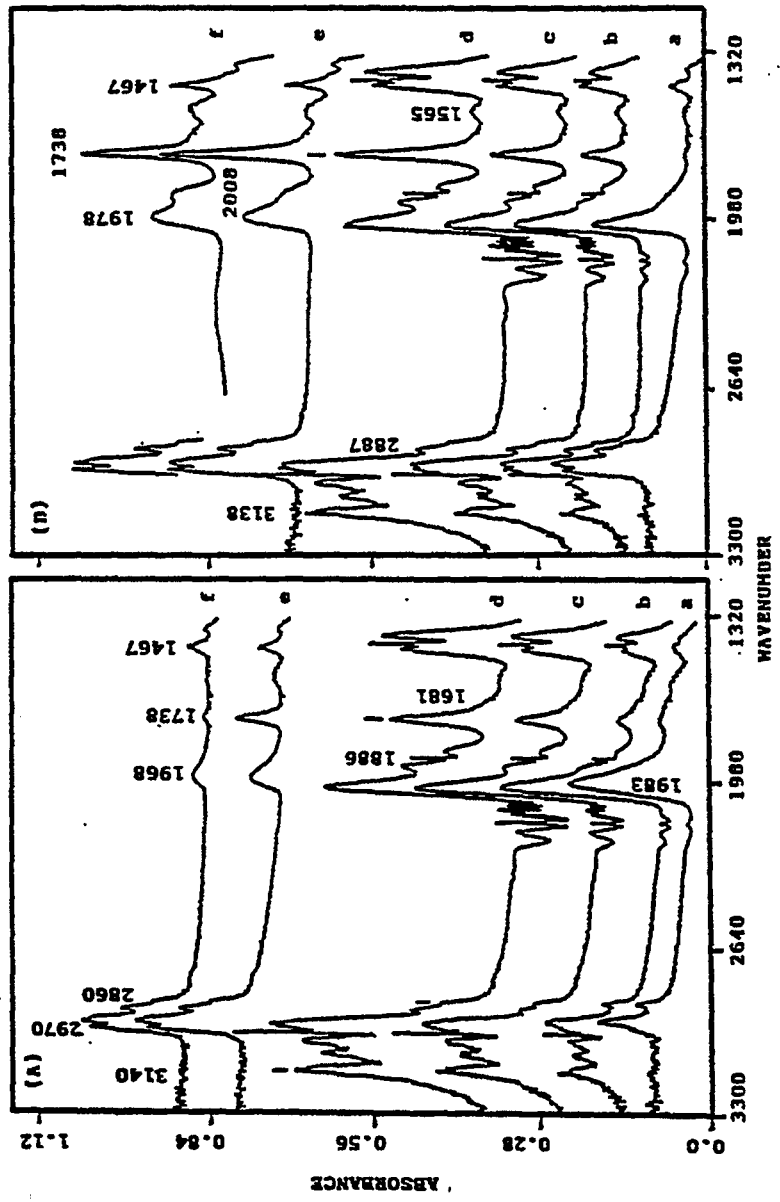


Figure 6.3 Infrared Spectra of CO/H₂/C₂H₄ Reaction at 513 K on (A) Ru/SiO₂ and (B) Sulfided Ru/SiO₂: (a) at 1 atm, (b) at 10 atm, (c) at 20 atm, (d) at 30 atm, (e) reduction in flowing H₂ at a rate of 5 cm³/min at 1 atm for 20 min, (f) for 10 hr.

listed in Table 6.2. At 1 atm, the linear CO was observed at 1983 ¹⁰¹ cm⁻¹. Increasing the total pressure resulted in an increase in the intensity of the linear CO band and an upward shift of the linear CO wavenumber. No obvious relation between CO insertion selectivity and the wavenumber of adsorbed CO was observed. The gaseous ethylene was observed at 1921, 1888, 1861 cm⁻¹, 1400-1500 cm⁻¹ and in the vicinity of 3100 cm⁻¹. One band at 1738 cm⁻¹ with a shoulder at 1681 cm⁻¹ began to emerge as reaction pressure increased. The former corresponds to adsorbed propionaldehyde, which was identified by the injection of the propionaldehyde to the Ru/SiO₂ catalyst and the SiO₂. It should be noted that the adsorption of propionaldehyde on both Ru/SiO₂ and SiO₂ produced the same IR band at 1738 cm⁻¹. How the adsorbed propionaldehyde is distributed on the surface of Ru and SiO₂ can not be determined from these IR results. The intensity of this band paralleled the rate of formation of the propionaldehyde. The shoulder at 1681 cm⁻¹ may be assigned to an acyl species [38,93]. The band has also been detected on Rh derived catalysts which exhibit high selectivity for C₂ oxygenate formation [38,60,93].

Admission of flowing H₂ to the reactor at 513 K removed the gas phase ethylene and ethane bands and gradually attenuated the intensity of the adsorbed CO band and propionaldehyde band. However, the hydrocarbon bands that resemble those observed in CO hydrogenation study did not readily desorb under the this reduction condition. This observation further supports the proposition that these species are situated on the support rather than on the metal surface.

Table 6.3 shows the effect of reaction pressure on the rate of product formation for CO/H₂/C₂H₄ on S-Ru/SiO₂. Ethane was the major product; methane and propionaldehyde were the minor products. A trace amount of C₃ hydrocarbons and acetaldehyde were also observed. Increasing reaction pressure led to increases in the rates of formation of all products. Increases in the ratio of C₂H₅CHO to C₂H₆ with increasing reaction pressures indicates that the formation of propionaldehyde is favorable at high pressures. Comparison of ratios of the formation rates of propionaldehyde and ethane before sulfidation to those after sulfidation shows that sulfur had a greater inhibition effect on the rate of the propionaldehyde formation than that of the ethane formation.

The influence of reaction pressure on the infrared spectra for the ethylene hydroformylation on S-Ru/SiO₂ are shown in Figure 6.3(B). The infrared bands for S-Ru/SiO₂ were similar to those observed for the Ru/SiO₂ catalyst. The hydrocarbon bands on the Ru/SiO₂ and the S-Ru/SiO₂ were identical in wavenumber and intensity. The intensity of the linear CO band was smaller on the sulfided catalyst. A relatively strong IR intensity of adsorbed propionaldehyde was also observed on the sulfided catalyst. Admission of flowing H₂ to the reactor led to a gradual decrease in the intensity of linear CO and a very slow reduction in the intensity of propionaldehyde. As compared to the Ru/SiO₂ catalyst, the propionaldehyde appeared to be strongly bonded on the S-Ru/SiO₂. As a result, the desorption of the adsorbed propionaldehyde from S-Ru/SiO₂ was greatly inhibited.

Table 6.3 CO/H₂/C₂H₄ Reaction over Sulfided Ru/SiO₂

	Pressure (atm)			
	1	10	20	30
Product Formation (mol/kg-hr)				
CH ₄	0.021	0.037	0.038	0.040
C ₂ H ₆	0.062	0.329	0.389	0.417
C ₃ HC	0.0006	0.002	0.003	0.005
CH ₃ CHO	0.00	0.008	0.005	0.009
C ₄ HC	0.00	0.005	0.018	0.021
C ₂ H ₅ CHO	0.00	0.039	0.081	0.011
C ₂ H ₅ CHO/C ₂ H ₆	0.00	0.118	0.208	0.264
C ₂ H ₅ CHO(S)/C ₂ H ₆ CHO ^a	0.00	0.134	0.154	0.171
C ₂ H ₆ (S)/C ₂ H ₆	0.289	0.267	0.327	0.252

Temperature: 315 K, CO:H₂:C₂H₄ = 1:1:1

The product with formation rate smaller than 1E-2 indicates a trace product

a: Ratio of the rate of the product formed on the sulfided Ru/SiO₂ to the rate of the product formed on the Ru/SiO₂

A careful comparison of the infrared spectra and rate data ¹⁰⁴ for the Ru/SiO₂ and the S-Ru/SiO₂ shows that adsorbed sulfur (i) slightly decreased the intensity and wavenumber of the linear CO band; (ii) inhibited desorption/reaction of linear CO in flowing hydrogen at 513 K; (iii) caused an emergence of the shoulder band of an unknown species at 1880-1890 cm⁻¹; (iv) increased the intensity of the propionaldehyde band; (v) suppressed the formation of CO hydrogenation products such as C₃, hydrocarbon and acetaldehyde; (vi) exhibited a more severe inhibition effect on the formation of propionaldehyde than the formation of ethane. The most interesting part of the above observations is the increase in the intensity of the propionaldehyde band and the decrease in the rate of formation of propionaldehyde with the addition of sulfur. The result suggests that sulfur appears to promote CO insertion but inhibit the desorption of propionaldehyde; therefore making desorption of propionaldehyde the rate-limiting step on the S-Ru/SiO₂.

6.3.6 Dynamic Behavior of Adsorbed Propionaldehyde

In order to determine the effect of adsorbed sulfur on the dynamic behavior of adsorbed propionaldehyde, a transient FTIR study was conducted by the following procedure. Following the steady-state hydroformylation at 10 atm and 513 K, the feed was switched from a steady-state flow of CO/H₂/C₂H₄ to a steady-state flow of CO/H₂. Figure 6.4-A shows a series of infrared spectra taken during the switch on the Ru/SiO₂. As CO/H₂ displaced CO/H₂/C₂H₄, the intensity of gaseous ethylene, adsorbed propionaldehyde, and acyl bands gradually decreased while the intensity and wavenumber of adsorbed CO increased. The displacement process for the gaseous ethylene is slow due to the

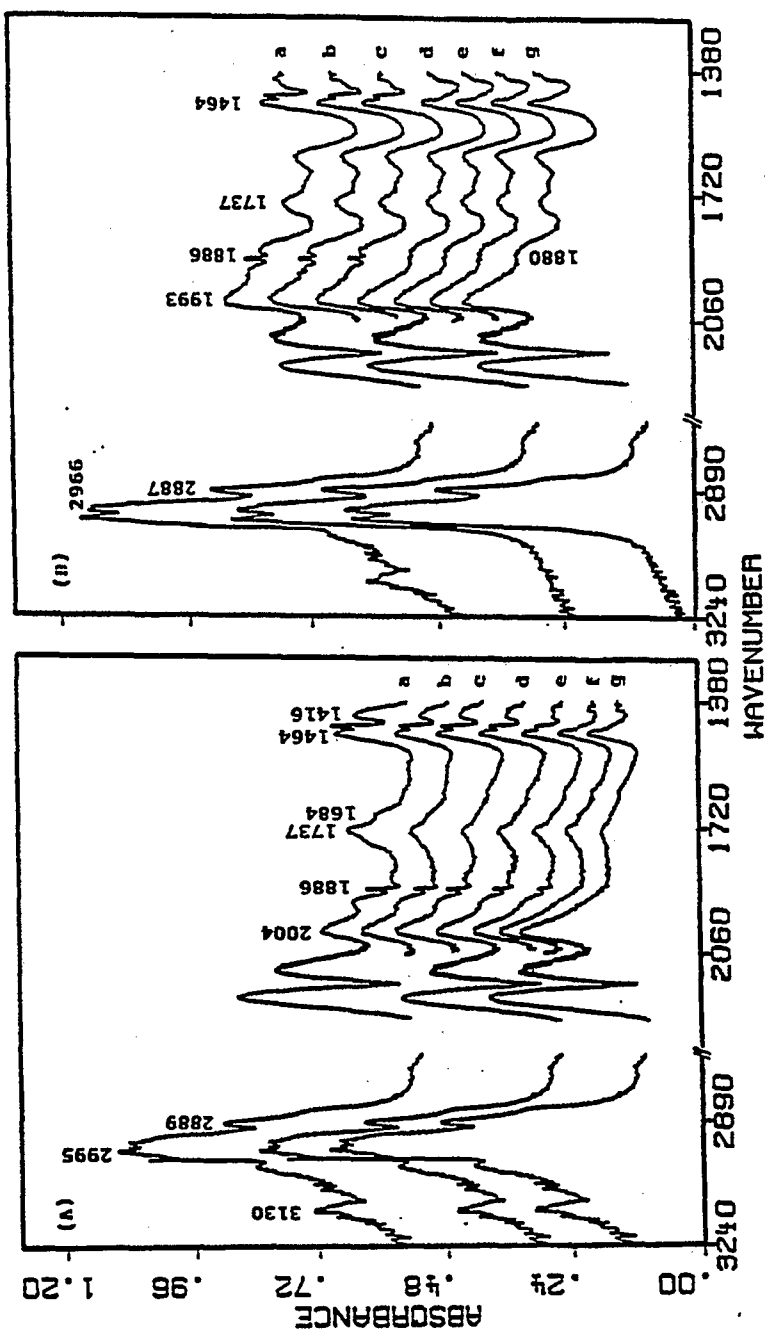


Figure 6.4 Transient Observation by Switching CO/H₂/C₂H₄ Flow to CO/H₂ Flow at 1 atm, 513 K on (A) Ru/SiO₂ and (B) Sulfided Ru/SiO₂: (a) steady state of CO/H₂/C₂H₄ reaction, (b) right after cut off C₂H₄ flow, (c) for 2 min, (d) for 4 min, (e) for 6 min, (f) for 15 min, (g) for 50 min.

condition of high pressure and the low flow rate even though the volume of the IR cell is 120 mm³.

Infrared spectra for the S-Ru/SiO₂ similar to those for the Ru/SiO₂ during the transient condition were also obtained as shown in Figure 6.4-B. The major difference in the spectra of adsorbed species on the Ru/SiO₂ and the S-Ru/SiO₂ during the switch is that the intensity of adsorbed propionaldehyde on the Ru/SiO₂ decreased much more rapidly than that of adsorbed propionaldehyde on the S-Ru/SiO₂. These results indicate that adsorbed propionaldehyde is more strongly bonded on the S-Ru/SiO₂ than on the Ru/SiO₂. As a result, the desorption of adsorbed propionaldehyde from S-Ru/SiO₂ is strongly inhibited, thus leading to the inhibition of the formation of gaseous propionaldehyde product from the hydroformylation.

6.3.7 Temperature Programmed Reaction with H₂

The reactivity of all the adsorbed species toward hydrogen was examined by temperature-programmed reaction with hydrogen. Prior to the TPR study, the CO/H₂/C₂H₄ reaction was carried out at 513 K and 10 atm for 1 hr to reach the steady state and then the reactor pressure and temperature were decreased to 1 atm and 298 K. Hydrogen was then passed through the reactor at a flow rate of 10 cm³/min; the reactor temperature was increased at a rate of 5 K/min.

Figure 6.5 shows a series of IR spectra taken during the TPR study. The initial spectrum at 298 K included the adsorbed linear CO, hydrocarbons, and propionaldehyde bands which are similar to those under reaction conditions. Band at 1672 cm⁻¹ that has been assigned to an acyl group was also observed.

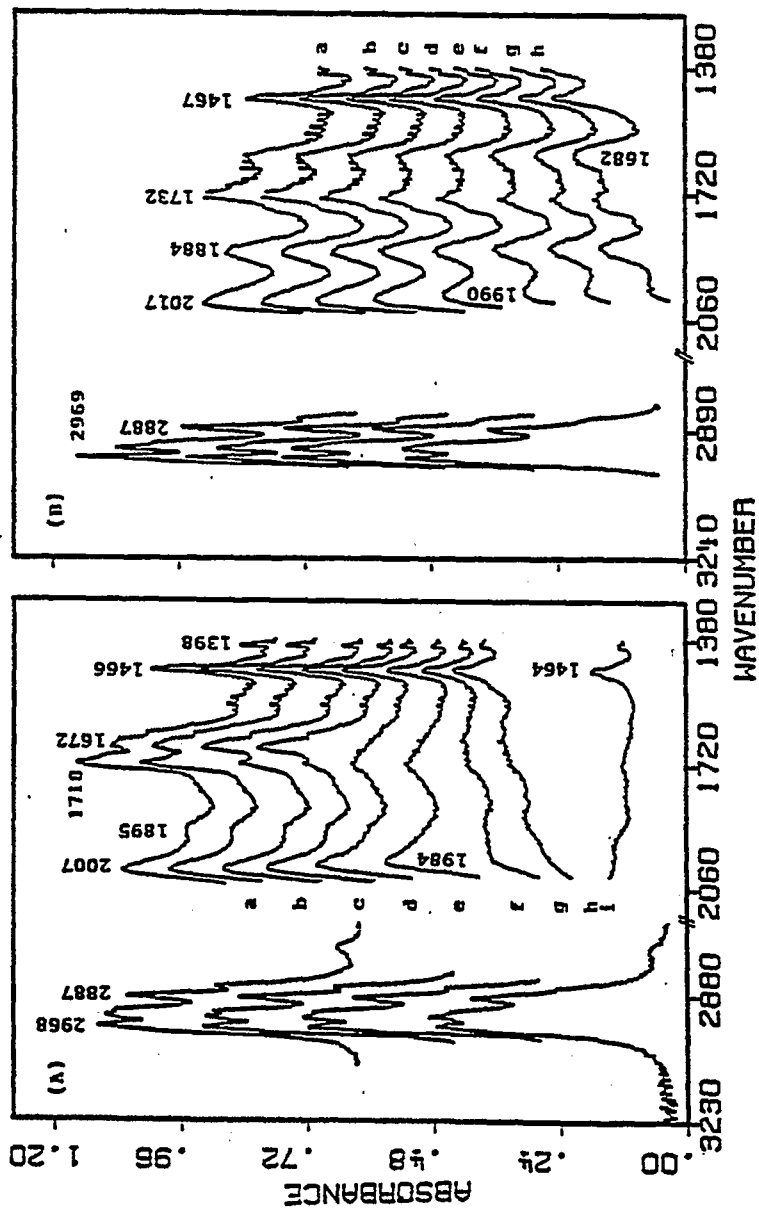


Figure 6.5 Temperature Programmed-Desorption of Adsorbed Species with Hydrogen (10 cm³/min) on (A) Ru/SiO₂ and (B) Sulfided Ru/SiO₂: (a) at 298 K, (b) at 323 K, (c) at 343 K, (d) at 373 K, (e) at 425 K, (f) at 473 K, (g) at 493 K, (h) at 513 K, (i) at 513 K for 10 hr.

In order to discriminate the change of intensity for CO and ¹⁰⁸ propionaldehyde bands with respect to temperature, a relative change in intensity of the bands was plotted as a function of temperature. The integrated absorbance is related to the concentration of the adsorbed species if the extinction coefficient is assumed to be independent of the surface coverage of the adsorbed species [31]. The integrated absorbance is defined as $\bar{A} = \int_{1932}^{2035} A(\nu)d\nu$, where ν is wavenumber. As shown in Figure 6.6, the intensity of integrated absorbance for the linear CO band on the Ru/SiO₂ showed a small decline from room temperature to 473 K and then followed by a rapid decrease as temperature increased above 473 K, while the intensity of the propionaldehyde band exhibited a rapid decrease to 423 K and then slowly depleted. In contrast, the intensity of the linear CO on the S-Ru/SiO₂ decreased linearly with increasing temperature, while the intensity of the propionaldehyde band showed an initial decline and then level off. These observations provide qualitative evidence that the linear CO is more strongly bonded on the Ru/SiO₂ than the S-Ru/SiO₂ at 303-480 K under flowing H₂ while the adsorbed propionaldehyde showed the reverse trend. By contrast, the more rapid diminishing of the linear CO on the Ru/SiO₂ than on the S-Ru/SiO₂ catalyst at 513 K under flowing H₂ (see Figure 6.2) may be explained by the easier of hydrogenation of adsorbed CO on the Ru/SiO₂ than on the S-Ru/SiO₂.

6.3.8 CO Hydrogenation and Ethylene Hydroformylation on the Washed Ru/SiO₂

Several recent studies have shown that an appreciable amount of residual chlorine (Cl) retains on the Ru/SiO₂ prepared from RuCl₃ [147,148]. Hydrogen reduction followed by hot-water washing is

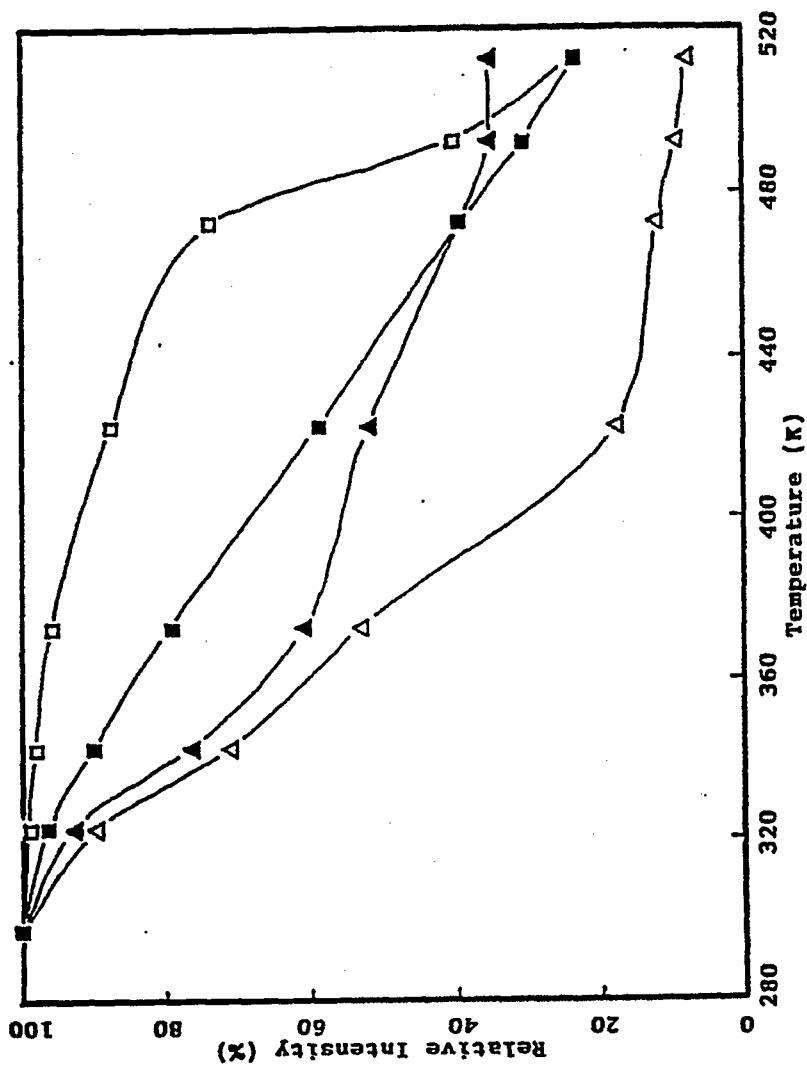


Figure 6.6 Relative Intensity Versus Temperature for the TPR of the Adsorbed CO and Propionaldehyde on Ru/SiO₂ and Sulfided Ru/SiO₂: Relative intensity is the ratio of the intensity of adsorbed species during TPR to the initial intensity of adsorbed species. (□) linear CO on Ru/SiO₂, (Δ) propionaldehyde on Ru/SiO₂, (■) linear CO on S-Ru/SiO₂, (▲) propionaldehyde on S-Ru/SiO₂.

required to remove Cl from the Ru/SiO₂ catalyst. Chlorine analysis ¹¹⁰ for the catalysts used in this study shows that the Ru/SiO₂ after hydrogen reduction contained 0.50 wt% Cl; the same sample which was washed by hot water (nearly boiled water) and reduced again at 673 K consisted of only 449 ppm Cl.

Figure 6.7 shows the infrared spectra of CO adsorption, CO hydrogenation, and ethylene hydrogenation on the hot-water washed Ru/SiO₂ at 513 K. The CO adsorption produced the band at 2044 cm⁻¹; the addition of hydrogen to CO resulted in the downward shift of the CO band and the formation of hydrocarbon bands at 2857 and 2927 cm⁻¹ at 10 atm. The addition of ethylene to the CO/H₂ mixture resulted in the further downward shift of the CO band as well as the appearance of propionaldehyde band at 1734 cm⁻¹ and hydrocarbon bands at 2889-3138 cm⁻¹. The infrared bands observed for adsorbed CO, propionaldehyde and hydrocarbons on the washed catalyst are in a good agreement with those reported for the Cl-containing Ru/SiO₂ (shown in Figure 6.1-6.3).

Chlorine appears to have little effect on the adsorption of CO on the Ru/SiO₂ catalysts. Comparison of the infrared spectra of CO adsorbed on the high and low Cl-containing catalysts (Figure 6.1-3 and 6.7) shows that the presence of Cl did not result in any significant changes in the wavenumber and intensity of CO band. The static chemisorption study revealed that CO uptake for the Cl-free Ru/SiO₂ is nearly equal to those for the Cl-containing catalyst; however, H₂ uptake for the Cl free Ru/SiO₂ is significantly higher than those for the Cl-containing catalyst [148,149]. Steady state transient kinetic analysis [150] showed that the presence of Cl decreased greatly the concentration of the CH_x surface intermediates without markedly

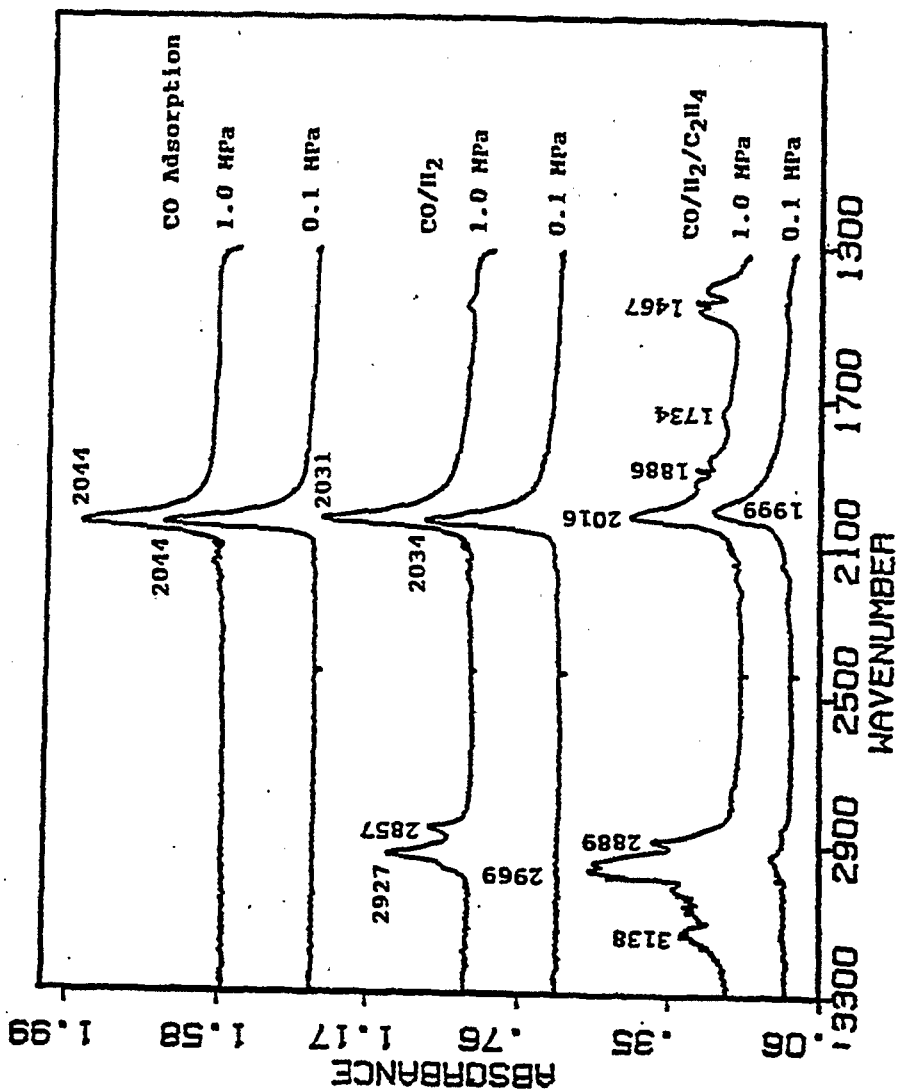


Figure 6.7 Infrared Spectra of CO Adsorption, CO/H₂, and CO/H₂/C₂H₄ Reactions on the Washed Ru/SiO₂ at 513 K.

affecting the coverage in CO under methanation conditions. These 112 results suggest that the major function of Cl is to depress hydrogen chemisorption that could lead to the suppression of hydrogenation.

Rates of product formation for CO hydrogenation and ethylene hydroformylation on the washed catalyst corresponding to IR data shown in Figure 6.7 are listed in Table 6.1 and 6.2. Low Cl-containing catalysts exhibited higher activity for hydrocarbon formation in CO hydrogenation as well as for ethane and propionaldehyde formation in ethylene hydroformylation than high Cl-containing catalyst. This could be partly attributed to high hydrogenation activity of the low Cl-containing catalyst that generates large quantity of C_nH_x ($n=1$ and 2) hydrocarbon intermediates for hydrogenation and CO insertion. The higher concentrations of hydrocarbon species on the lower Cl-containing Ru/SiO₂ can also be clearly discerned from the comparison of IR spectra of adsorbed CO in Figure 6.2, 6.3, and 6.7 that shows higher intensity of hydrocarbon bands on the low Cl-catalyst.

6.4 Conclusions

Although olefin hydroformylation has been well recognized as homogeneously catalyzed reaction, the presence of linearly adsorbed CO and adsorbed propionaldehyde and the absence of Ru carbonyl species on the surface of the Ru catalysts suggest that the ethylene hydroformylation can also occur on the surface of the Ru/SiO₂ catalyst. Increases in reaction pressure enhance the selectivity to propionaldehyde on both Ru/SiO₂ and S-Ru/SiO₂ catalysts. However, reaction pressure has little effect on the infrared spectra of CO adsorbed on the catalysts. The effect of sulfur on the reaction on Ru/SiO₂ can be summarized as follows:

- (i) Sulfur blocked bridge CO sites and inhibited the desorption of adsorbed propionaldehyde.
- (ii) Sulfur poisoned the formation of higher hydrocarbons and oxygenates in CO hydrogenation.
- (iii) Sulfur poisoned ethylene hydrogenation and hydroformylation.

This is in contrast to our previous observations that adsorbed sulfur is ineffective in poisoning ethylene hydroformylation on the Rh/SiO₂ catalyst; adsorbed sulfur promotes hydroformylation on the Ni/SiO₂. While sulfur poisons indiscriminately Group VIII metals for CO hydrogenation, it exhibits different poison and promotion effects on the Ru, Rh, and Ni metals for hydroformylation. The poisoning effect of sulfur on hydroformylation on the Ru/SiO₂ has been ascribed to an inhibition of desorption of the adsorbed propionaldehyde brought about by adsorbed sulfur.

The presence of residual chlorine on the Ru/SiO₂ catalyst was found to affect slightly the infrared spectra of adsorbed CO but to reduce appreciably the activity of the catalyst for the hydrocarbon formation.

CHAPTER VII

THE EFFECT OF SILVER PROMOTION ON CO HYDROGENATION AND ETHYLENE HYDROFORMYLATION OVER Rh/SiO₂ CATALYSTS

7.1. Introduction

Carbon monoxide hydrogenation over Rh catalysts produces a wide range of products including hydrocarbons, alcohols, aldehydes, and acids [8,20]. Several studies have shown that the selectivity of Rh catalyst greatly depends on the compositions of supports and promoters. Formation of methanol over Rh is enhanced by use of ZnO, CsO, and MgO as supports [44,47]. Rh on pure SiO₂ and Al₂O₃ supports produces mainly hydrocarbons while Rh on TiO₂ and La₂O₃ produces primarily acetaldehyde and ethanol [10-12,60]. Promoters, including Mn, Zr, Ti, V and La oxides, have been demonstrated to enhance C₂ oxygenate selectivity over Rh catalysts [38,78]. A selective inhibition effect of alkali promoters on hydrogenation leads to the enhancement of C₂ oxygenate selectivity [79-82].

The modification of catalyst activity and selectivity by various promoters has been summarized as follows: (i) blockage of surface sites by the presence of additives, (ii) interaction of additives with reactant molecules, and (iii) modification of the catalyst by the electronic effect of additives. Physical blockage of the surface active site by additives, such as Zn and Fe, have a great

effect on CO dissociation which require large ensembles of surface atoms [84-86]. The oxophilic ions such as Mn, Ti, and Zr tend to interact with oxygen atom of CO and oxygenate intermediates and to stabilize these surface species [39,64,83,92]. The electronic effects of the additives, especially that of alkali-promoted metals, are known to increase CO adsorption energy and the CO dissociation activity and to suppress hydrogenation of surface carbon [81,82].

Ag, for which electronegativity is similar to that of Rh metal, is an inactive compound for a number of reactions including CO hydrogenation, olefin hydrogenation, and alkane hydrogenolysis [98]. Depending on the structure sensitivity of the reactions and distribution of inert additives on the surface of an active metal, the addition of the inactive component such as Ag may not only modify the overall activity but also change the selectivity of the reaction. This paper reports results of the CO hydrogenation and ethylene hydroformylation on Ag-Rh/SiO₂ catalysts. Emphasis was placed on the effect of reaction pressure and the concentration of Ag on the C₂₊ oxygenate selectivity.

7.2 Experimental

7.2.1 Catalyst Preparation and Characterization

Three wt% Rh/SiO₂ was prepared by impregnation of SiO₂ (Strem Chemicals) using Rh nitrate (Alfa Chemicals). Ag-Rh/SiO₂ was prepared by coimpregnation using both Rh and Ag nitrates. The percentage of Rh is the same for all Ag-Rh/SiO₂ catalysts. The molar ratios of Ag to Rh are 0.25, 0.5, and 1. The Ag(1)Rh/SiO₂ catalyst was denoted as the catalyst with the Ag/Rh ratio of 1; the Ag(0.5)Rh/SiO₂ catalyst was represented by the catalyst with the Ag/Rh ratio of 0.5; and the

Ag(0.25)Rh/SiO₂ catalyst was denoted as the catalyst with the Ag/Rh¹¹⁶ ratio of 0.25. After impregnation, the samples were dried overnight in air at 313 K, then reduced in flowing hydrogen at 673 K for 16 hr.

Infrared spectroscopy of chemisorption of CO and NO and X-ray photoelectron spectroscopy (XPS) were employed to study the surface structure and the surface state of the catalysts. Chemisorption of CO and NO on the Rh/SiO₂ and Ag-Rh/SiO₂ was studied in an IR cell at 301 K and 1 atm. Gas phase CO bands were eliminated by subtracting the absorbance of gas phase CO with a SiO₂ disk in the cell from the spectra of adsorbed species on the Rh/SiO₂ and Ag-Rh/SiO₂ catalysts.

7.2.2 Experimental Procedure

CO hydrogenation and ethylene hydroformylation were performed over the catalysts in the IR cell under 513 K and 10-20 atm. The details of experimental procedures have been reported in Chapter III.

7.3 Results

7.3.1 X-Ray Photoelectron Spectroscopy

Figure 7.1 shows the XPS spectra of Rh/SiO₂ and Ag-Rh/SiO₂ taken after reduction at 513 K. The Rh 3d_{3/2} and 3d_{5/2} bonding energies for the Rh/SiO₂ catalyst were observed at 311.4 and 306.7 eV, respectively. The presence of Ag on Rh/SiO₂ caused an upward shift of the Rh 3d_{3/2} and 3d_{5/2} binding energies to 312 and 307 eV and a decrease in the intensity ratio of Rh to Ag peaks. Our recent study showed that following the oxidation at 513 K, the Rh 3d_{3/2} and 3d_{5/2} binding energy shifted to 307.5 and 312.3 eV which as been assigned to Rh⁺ ion. Comparison of Rh binding energy of the reduced Rh, oxidized Rh, and Ag-Rh catalysts shows that the oxidation state of Rh on Ag-Rh/SiO₂ catalyst is between 0 and +1 after reduction. The decrease

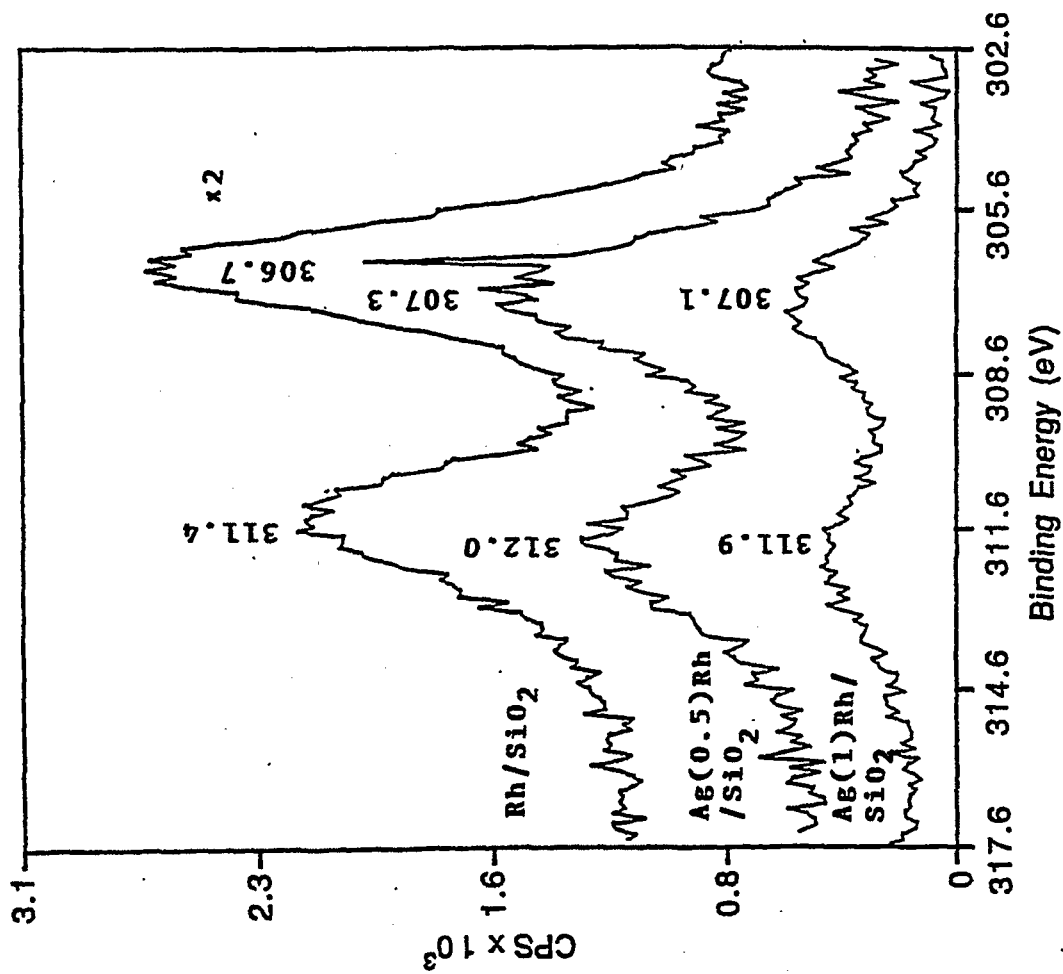


Figure 7.1 Rh 3d_{5/2}, 3d_{3/2} XPS Spectra of Rh/SiO₂ and Ag-Rh/SiO₂ Catalysts

in the intensity ratio of Rh to Ag peaks indicates that Rh surface is partly covered by Ag on the Ag-Rh/SiO₂ catalysts. 118

7.3.2 CO Adsorption

Figure 7.2 shows the infrared spectra of CO adsorption on Rh/SiO₂ catalysts with different Ag loading at 301 K and 1 atm. Two bands at 2060 and 1874 cm⁻¹ over the Rh/SiO₂ catalyst are assigned to linear and bridged CO on the reduced Rh metal [119,120,123], respectively. IR study on Ag/SiO₂ shows that CO adsorption on Ag/SiO₂ did not produce adsorbed CO species. The presence of Ag on Rh/SiO₂ decreased the wavenumber of linear CO band and the intensity ratio of the bridge CO to linear CO band. These results clearly indicate that Ag additives reduced interactions between adsorbed CO and blocked bridge CO sites.

As Ag/Rh ratio increased to 1, a new band at 2090 cm⁻¹ emerged. The 2090 cm⁻¹ band may be assigned to linear CO adsorbed on the Rh⁺ ions. Linear CO adsorbed on Rh⁺ is known to give an IR band in the 2100-2090 cm⁻¹ region [17,119,123]. The XPS results further confirm the possible presence of Rh⁺ ion on the surface of the Ag-Rh/SiO₂.

7.3.3 NO Adsorption

Infrared spectrum of NO adsorption on silica at room temperature, as shown in Figure 7.3, displays the IR bands at 1875 cm⁻¹ with two asymmetric R and P branch at 1903 and 1850 cm⁻¹, respectively. Increasing the pressure of NO increases the intensity of the P branch and forms a new band near 1600 cm⁻¹. Purge of nitrogen flow immediately removes all of these IR bands of NO.

Figure 7.4 shows infrared spectra of NO adsorption on Rh/SiO₂ catalysts with different Ag loading. In Table 7.1 the wavenumbers and

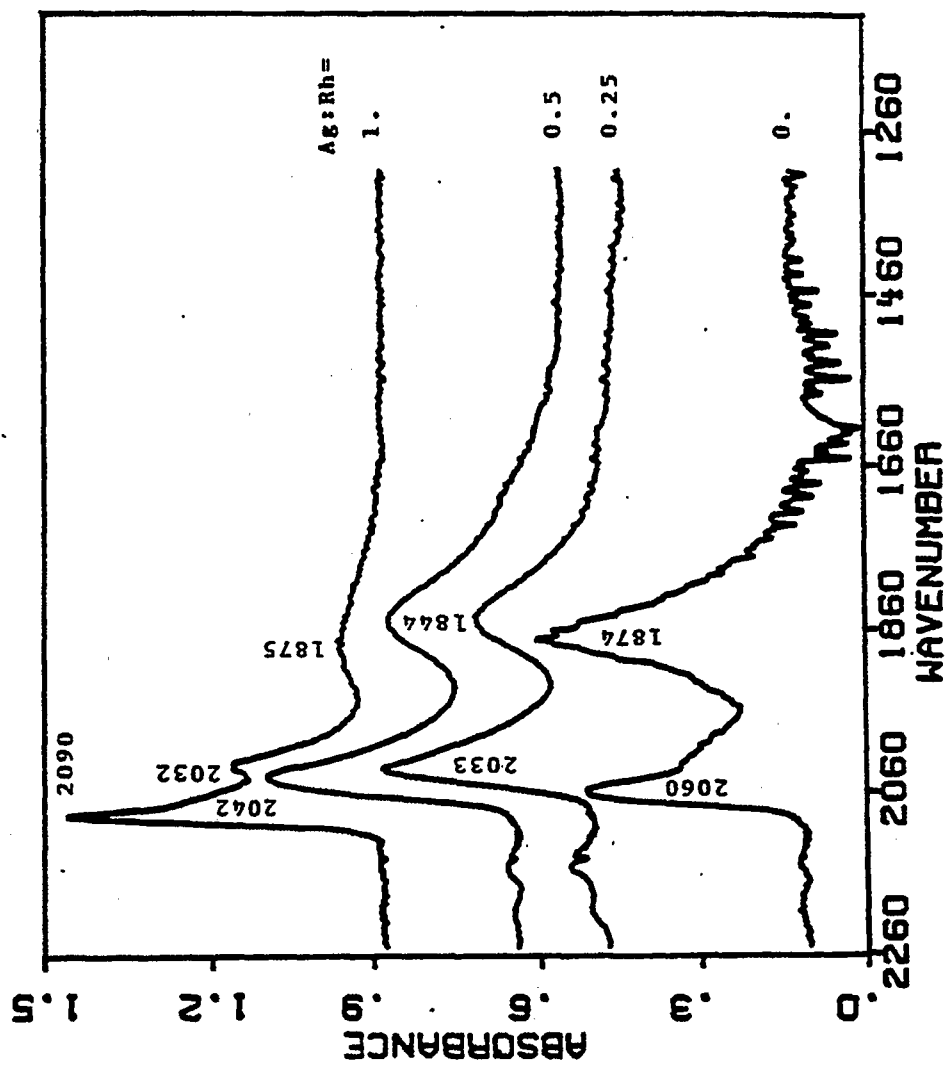


Figure 7.2 Infrared Spectra of CO Adsorption on Rh/SiO₂ and Ag-Rh/SiO₂ at 301 K.

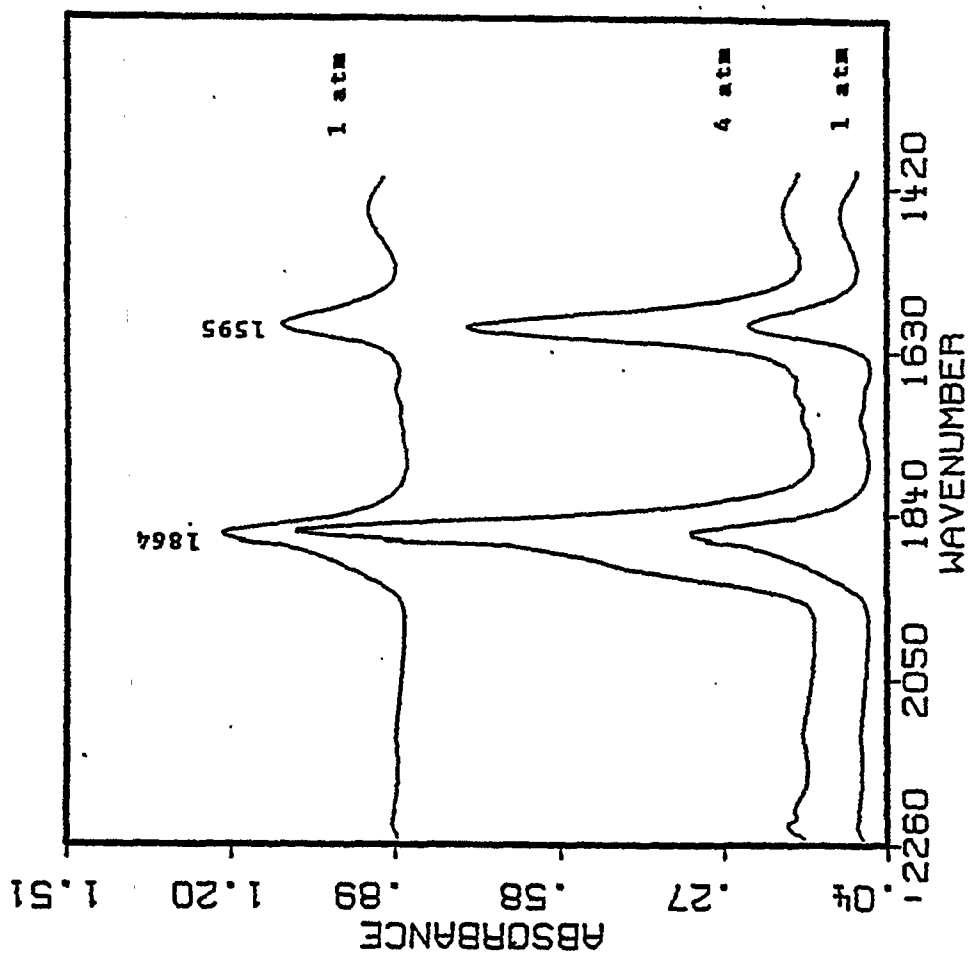


Figure 7.3 Infrared Spectra of NO Adsorption on Silica at 301 K.

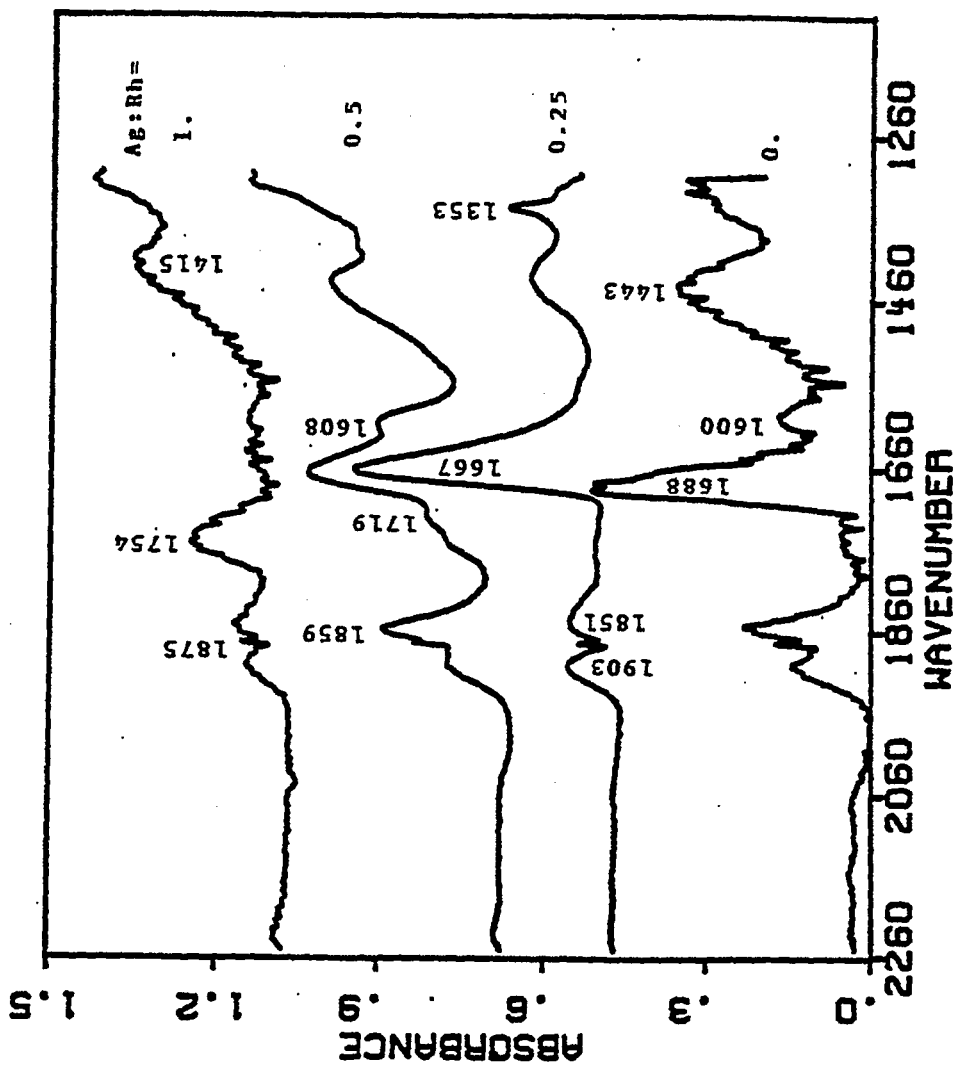


Figure 7.4 Infrared Spectra of NO Adsorption on Rh/SiO₂ and Ag-Rh/SiO₂ at 301 K.

Table 7.1 Assignment of Infrared Bands for Adsorbed NO

Catalyst	M-NO ⁺	M-NO	M-NO ⁻	Ref.
Rh/SiO ₂	1920-1910	1800-1795	1680-1660	151
Rh/SiO ₂	-	1810-1790	1690-1630	152
Rh/Al ₂ O ₃	1910	1830	1755-1655	153
Rh/Al ₂ O ₃	1920	1838	1740-1660	154
K-Rh/Al ₂ O ₃	1910	1825	1730	155
Ru/SiO ₂	1815		1760	156

assignments of the bands found in the infrared spectra obtained for ¹²³ NO adsorption on different catalysts are shown [152-156]. As shown in Figure 7.4, the band in the 1754-1667 cm⁻¹ region can be assigned to surface anionic NO (NO⁻); the band in the 1443-1415 cm⁻¹ region is characteristic of nitrate species such as NO₂⁻ and NO₃⁻ [153,154]. The bands at 1903, 1875, 1851, and 1608 cm⁻¹ are similar to the IR bands obtained from NO adsorption on silica. These bands were completely removed in the flow of nitrogen while the bands of surface NO⁻ nitrate species remain unchanged. A band near 1719 cm⁻¹ emerged as a shoulder of the NO⁻ band as the Ag/Rh ratio increased. Increasing the Ag/Rh ratio to 1 resulted in formation of a band near 1754 cm⁻¹ and the NO⁻ band at 1667 cm⁻¹ disappeared. Comparison of the wavenumber of the adsorbed NO species indicates that NO adsorbed on the Ag-Rh/SiO₂ may be assigned to partial negative NO species, NO^{δ-}, which exhibits wavenumber between ν_{NO} and ν_{NO^-} .

7.3.4 CO Hydrogenation

Figure 7.5 shows the infrared spectra for CO hydrogenation. The rates of product formation corresponding to the infrared spectra are presented in Table 7.2. Methane was the major product; acetaldehyde and C₂-C₃ hydrocarbons were the minor product over the Rh/SiO₂ catalyst at 513 K and 10 atm. Under the same condition, the infrared spectrum shows linear CO and bridged CO bands at 2035 cm⁻¹ and 1843 cm⁻¹, respectively.

The presence of Ag on Rh/SiO₂ led to a decrease in the rates of methane and ethane formation but the formation rate of acetaldehyde was varied. Our extended study [157] in CO hydrogenation over Ag-Rh/SiO₂ with wide reaction temperature has shown that the selectivity for

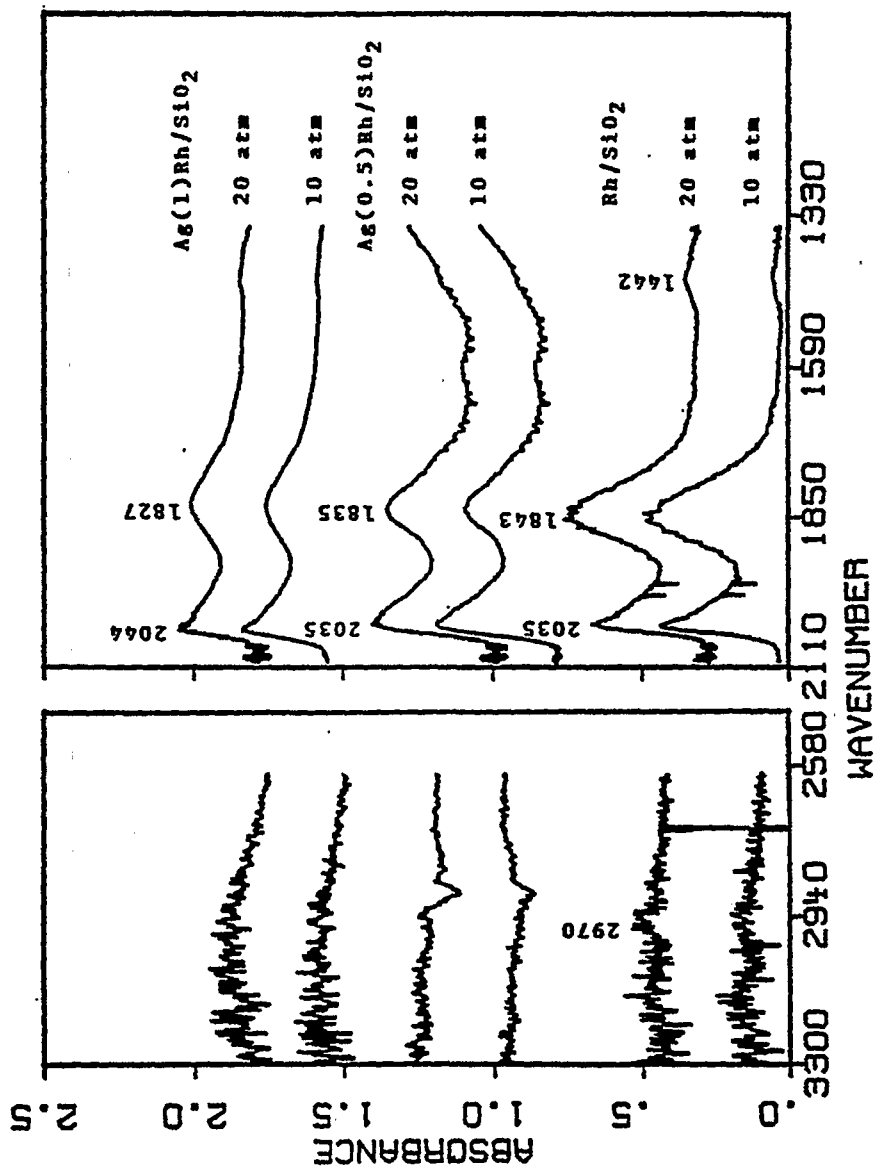


Figure 7.5 Infrared Spectra of CO Hydrogenation on Rh/SiO₂ and Ag-Rh/SiO₂.

Table 7.2 Rates of Product Formation of CO Hydrogenation at 513 K

Catalyst	Pressure (atm)	Rate of product formation (mol/Kg-hr)						$\frac{\text{CH}_3\text{CHO}^a}{\text{CH}_4}$
		CH ₄	C ₂ H ₄	C ₂ H ₆	C ₃ H ₈	CH ₃ CHO	CH ₄	
Rh/SiO ₂	10	0.403	0.006	0.167	0.003	0.015	0.037	
	20	0.470	0.099	0.153	0.005	0.018	0.038	
Ag(0.5)Rh/ SiO ₂	10	0.144	0.003	-	-	0.002	0.014	
	20	0.156	0.048	0.001	-	0.013	0.076	
Ag(1)Rh/ SiO ₂	10	0.168	0.060	0.005	0.024	0.025	0.148	
	20	0.161	0.073	0.003	0.022	0.079	0.491	

a: molar ratio of CH₃CHO and CH₄.

acetaldehyde increases with increased silver. Infrared spectra corresponding to rate data shows that increasing the Ag/Rh ratio decreased the ratio of intensity of bridge and linear CO bands. However, the extent of decrease in the intensity ratio of bridge CO to linear CO band brought about by Ag is smaller for the catalysts under CO hydrogenation conditions than those under CO adsorption at 301 K. Increasing reaction pressure from 10 to 20 atm increased the rate and selectivity for acetaldehyde formation, but did not change the infrared spectra of adsorbed CO. The intensity of hydrocarbon bands were small compared to that of adsorbed CO and no acetaldehyde band was observed. The linear CO band on the Rh⁺ site was not observed on the Ag(1)Rh/SiO₂ catalyst under reaction conditions.

7.3.5 Ethylene Hydroformylation

Figure 7.6 shows infrared spectra of ethylene hydroformylation. The rates of product formation corresponding to the infrared spectra are presented in Table 7.3. Ethane and propionaldehyde were the major products; methane and acetaldehyde were the minor products over the Rh/SiO₂ catalyst at 513 K and 10 atm. Under the same reaction condition, the infrared spectra shows linear CO band in the 2025-2020 cm⁻¹ region. The bridged CO band is overlapped by gaseous ethylene at 1919, 1888, and 1850 cm⁻¹. The band at near 1730 cm⁻¹ has been assigned to propionaldehyde [41]. The infrared spectrum in the 3140-2700 cm⁻¹ region is due to hydrocarbon species. The bands at 3138 and 3067 cm⁻¹ are exhibited by gaseous ethylene [134]; the band at 2899 cm⁻¹ is due to gaseous ethane [135]; and the band at 2720 cm⁻¹ is characteristic of the C-H stretching of propionaldehyde [41].

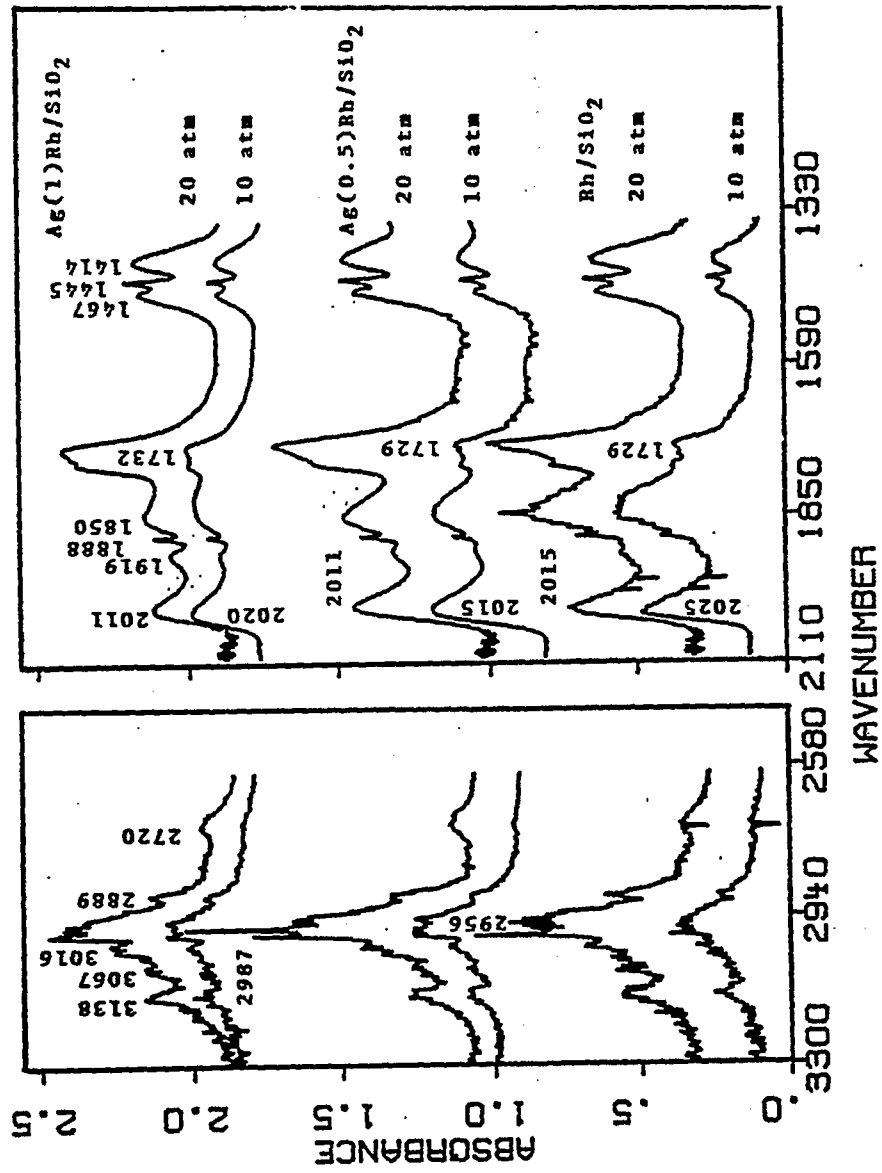


Figure 7.6 Infrared Spectra of Ethylene Hydroformylation on Rh/SiO₂ and Ag-Rh/SiO₂.

Table 7.3 Rates of Product Formation of Ethylene Hydroformylation at 513 K

Catalyst	Pressure (atm)	Rate of produce formation (mol/Kg-hr)						$\frac{C_2H_5CHO^a}{C_2H_6}$
		CH ₄	C ₂ H ₆	C ₃ HC	CH ₃ CHO	C ₂ H ₅ CHO	C ₂ H ₆	
Rh/SiO ₂	10	0.194	36.9	0.012	0.013	10.6	0.287	
	20	0.168	34.3	0.010	0.007	13.1	0.382	
Ag(0.5)Rh/ SiO ₂	10	0.066	31.7	0.029	0.011	18.3	0.577	
	20	0.071	35.4	0.039	0.012	28.8	0.814	
Ag(1)Rh/ SiO ₂	10	0.067	27.5	0.072	0.009	20.1	0.731	
	20	0.069	24.8	0.076	0.013	25.3	1.02	

a: molar ratio of C₂H₅CHO and C₂H₆.

The presence of Ag on Rh/SiO₂ suppressed the rates of methane and ethane formation but enhanced the rate of propionaldehyde formation. The presence of Ag also significantly reduced the intensity of bridge CO bands but slightly decreased the intensity of linear CO bands. Increasing reaction pressure from 10 to 20 atm increased the formation rate of propionaldehyde and the selectivity toward propionaldehyde. The increase in pressure reduced wavenumber but increased the intensity of the linear CO band and increased the intensity of hydrocarbon and propionaldehyde bands. The decrease in wavenumber of the linear CO band has been attributed to a decrease in the dipole-dipole coupling as a result of the dilution of adsorbed CO by adsorbed propionaldehyde and hydrocarbons [118].

7.4 Discussion

7.4.1 Catalyst Characterization

Table 7.4 summarizes the results of XPS, IR of adsorbed CO and NO together with previous results in H₂ chemisorption and X-ray diffraction studies. The small variation of H₂ chemisorption to Ag/Rh ratio indicates that surface area of Rh particle was not greatly affected by the presence of Ag additives. XRD results suggested that most of the Ag form aggregates on the SiO₂ supports. The effect of Ag on the surface of Rh crystallites can be elucidated from results of XPS and infrared spectra of CO adsorption. XPS results indicates an upward shift of the binding energy and high Ag/Rh peak intensity ratio when Ag was added to Rh/SiO₂. The high intensity ratio of XPS peak of Ag/Rh suggests that a fraction of Ag covers the surface of the Rh metal crystallite. The presence of Ag on the surface of Rh crystallites of Ag-Rh/SiO₂ can be further confirmed by the low intensity ratio of

Table 7.4 Catalyst Characterization for Various Ag/Rh Ratio

Ag/Rh Ratio	XPS (eV) 3d _{5/2} 3d _{3/2}	Ag/Rh ^a XPS Peak	CO Adsorption (cm ⁻¹)	B/L ^b Ratio	NO Adsorption (cm ⁻¹)	Crystal. Size (A°) Rh (H ₂ Chem.)	Ag/Rh (XRD)	H ₂ Chem. μ mol/g
0	311.4 306.7	-	2060,1840	1.23	1754,	96 ^c	-	13.7
0.5	312.0 307.3	0.26	2040,1844	0.51	1720,1667	97	468/85	13.5
1.0	311.9 307.1	0.79	2090,2030,1875	0.33	1688	100	395/136	12.9

a: Intensity ratio of XPS peak of Ag to Rh.

b: Intensity ratio of bridge CO band to linear CO band.

c: Average particle size was estimated from H₂ chemisorption, assuming the ratio of H₂-to-Rh to be 1 and the particle to be cubic with five sides exposed to hydrogen.

bridge to linear CO band for the Ag-Rh/SiO₂. Ag appears to disperse on the surface of Rh crystallite resulting in the blocking of bridged CO sites. The change in the ratio of intensities of bridged and linear CO bands is similar to those reported for Zn- and Fe-promoted Rh/SiO₂ [83-86].

In addition to Ag modification of structure of Rh surface, Ag influenced the electronic state of Rh surface. The binding energy for the Rh 3d_{3/2} and 3d_{5/2} were shift from 311.4 and 306.7 eV for Rh/SiO₂ to 312 and 307 eV for Ag-Rh/SiO₂ indicating that the surface of Ag-Rh/SiO₂ contains more Rh⁺ than that of Rh/SiO₂. The presence of Rh⁺ on the Ag-Rh/SiO₂ gave prominent CO band at 2090 cm⁻¹ as shown in Figure 7.2. The absence of tilted CO in infrared spectra of CO chemisorption suggests that the presence of Ag did not directly interact with oxygen atom of adsorbed CO.

NO chemisorption also reveals the effect of Ag on the Rh/SiO₂ catalyst. Adsorbed NO has shown a remarkable sensitivity in vibration frequency to the electronic state of the surface. Variety of forms, ranging from NO⁻ to NO⁺, has been assigned [151-156]. The bent-type M-NO⁺ is formed by electron donation from the metal to antibonding orbital of NO molecule; the linear-type M-NO⁻ is formed by electron withdraw from NO. The formation of NO^{δ-} band in addition to the NO⁻ band in the presence of Ag (shown in Figure 7.4) indicated that the presence Ag might form Rh⁺ ions which may vary NO⁻ to NO^{δ-}. The formation of Rh⁺ is confirmed with the observation of linear CO on the Rh⁺ site.

As shown in Table 7.2, the presence of Ag increased the rate of acetaldehyde formation and slightly increased the rate of ethane and ethylene formation but decreased the rate of methane formation. It has been proposed that CO dissociates forms surface carbon which then hydrogenates to CH_x hydrocarbon intermediates [23-31]. The hydrocarbon intermediate may undergo hydrogenation to methane, CH_x insertion to ethane or ethylene, or CO insertion to acetaldehyde [32-40]. The increase in the rate of acetaldehyde formation and the molar ratio of acetaldehyde to methane indicates that the presence of Ag enhanced the catalyst activity in CO insertion.

Increasing reaction pressure enhanced the formation rate of propionaldehyde, especially on the Ag-promoted Rh/SiO₂ catalysts which indicates that high pressure of CO enhances CO insertion.

The results of ethylene hydroformylation further confirm the effect of Ag on enhancement of C₂ oxygenate synthesis. Hydrogenation of adsorbed ethylene forms surface ethyl species. The presence of Ag enhances the catalyst activity of CO insertion into the ethyl species leading to increase in the formation of propionaldehyde (shown in Figure 7.6). Increase in the Ag/Rh ratio also decreased the rate of ethylene formation indicating that Ag suppressed hydrogenation.

7.5 Conclusions

The results of XRD, XSP, H₂ chemisorption, and infrared spectra of CO and NO adsorption reveal that part of Ag formed aggregate on silica support and that a fraction of Ag dispersed on the Rh metal surface. IR indicates that the major effect of Ag is to block the bridge CO sites on the Rh surface.

Ag exhibited great effect on CO hydrogenation and ethylene 133
hydroformylation. The presence of Ag increased the rate and
selectivity of acetaldehyde formation in CO hydrogenation and the rate
and selectivity of propionaldehyde formation in ethylene
hydroformylation. The increased C₂₊ oxygenate synthesis activity for
Ag-Rh/SiO₂ which possesses high concentration of linear CO sites
indicates that the single Rh site is active for CO insertion.

CHAPTER VIII
THE EFFECT OF CHEMICAL ADDITIVES ON CO HYDROGENATION
AND ETHYLENE ADDITION OVER Rh/SiO₂ CATALYSTS

8.1 Introduction

One effective approach to enhancing the catalyst activity and selectivity is the use of chemical additives as catalyst modifiers. Extensive studies have been devoted to investigating the effect of chemical additives (promoters and poisons) and supports on the activity and selectivity of Rh for C₂ oxygenate synthesis [20,22,39,57,59,60,82,163,164,167]. Studies on the support effect on CO hydrogenation have shown that Rh on MgO, a basic support, exhibits a 90% selectivity to methanol [60]. The use of an acidic support, such as Al₂O₃, results mainly in CH₄, while the use of a slightly acidic or basic support (e.g. SiO₂, TiO₂, and CeO₂) produces both higher alcohols and hydrocarbons. Due to the complication from the support effect, identification of the role of additives in the C₂ oxygenate synthesis on supported Rh has been a challenging subject.

The objective of this work was to investigate the influence of various additives on the activity and selectivity of Rh/SiO₂ for higher oxygenate synthesis. SiO₂ was employed for this study due to its inertness. The use of SiO₂ as a support could minimize the possible complications and effects from the support. The additives Cu, Ag, P,

and S, which have different electronegativities, were chosen for this study. CO hydrogenation over the Rh-based catalyst were studied at 1.01 MPa and 573 K, in which the formation of higher oxygenates is highly favorable. Ethylene addition was employed as a probe reaction to investigate the effect of the chemical additive on the specific reaction steps, i.e. hydrogenation, CO insertion, chain incorporation, and hydrogenolysis. The performance of catalysts with the additives were compared with a Rh catalyst with no additive. The results of this work will be summarized and compared to other additives reported in the literature.

8.2 Experimental

8.2.1 Catalyst Preparation

Unpromoted 3 wt% Rh/SiO₂ was prepared by incipient wetness impregnation of SiO₂ (Strem Chemicals) using RhCl₃·3H₂O (Alfa Products). The catalysts P-Rh/SiO₂, Cu-Rh/SiO₂, and Ag-Rh/SiO₂ were prepared by using co-impregnation of P₂O₅, Cu(NO₃)₂·3H₂O, and AgNO₃ (all from Alfa Products), respectively. The ratio of additive to Rh is 1:2 and the same amount of Rh/SiO₂ was used as the unpromoted catalyst. After impregnation, all the samples were dried overnight in air at 313 K and then reduced in flowing hydrogen at 673 K for 16 hours. The sulfur additive was added by passing 1000 ppm H₂S in H₂ through the catalyst bed at 673 K for 2 hours.

8.2.2 Experimental Procedure

CO hydrogenation (CO/H₂ = 1) over the Rh-based catalysts were carried out in a differential reactor system at 573 K and 1.01 MPa. The space velocities were controlled in the range of 1100 to 11,000

hr⁻¹ to keep the CO conversion below 5% to minimize heat and mass transfer effects and secondary reactions. The product distribution was analyzed by an HP-5890A gas chromatograph with a 6 feet porapak PS column in series with a 6 feet porapak QS column. This combination permits a good on-line separation of methane and C₂-C₆ paraffins and olefins as well as C₁-C₄ oxygenates.

Ethylene was employed as a probe molecule to investigate the effect of the additive on specific reaction steps. The addition of ethylene to syngas was performed under the same conditions as the CO hydrogenation reaction. The addition of ethylene to the reactant stream was controlled at 2-15 mol%. The added ethylene produces an adsorbed ethyl species which can undergo the following specific reaction steps: 1) hydrogenation to ethane; 2) CO insertion to propionaldehyde, 3) chain incorporation to form higher hydrocarbons, 4) hydrogenolysis to methane [39,55,82,114,161]. The activity and selectivity of the catalyst for a specific reaction step were examined by comparing the product distribution before and after ethylene addition.

8.3 Results and Discussion

Due to the heterogeneity of the surface of promoted Rh catalyst and lack of knowledge on the site actually participating in the reactions, the reaction rate will be reported on the basis of mole/kg-hr rather than turnover number. Selectivity will be of major concern.

Figure 8.1 shows the rate of CO conversion and selectivities of the products of the CO hydrogenation reaction. Methane, olefins,

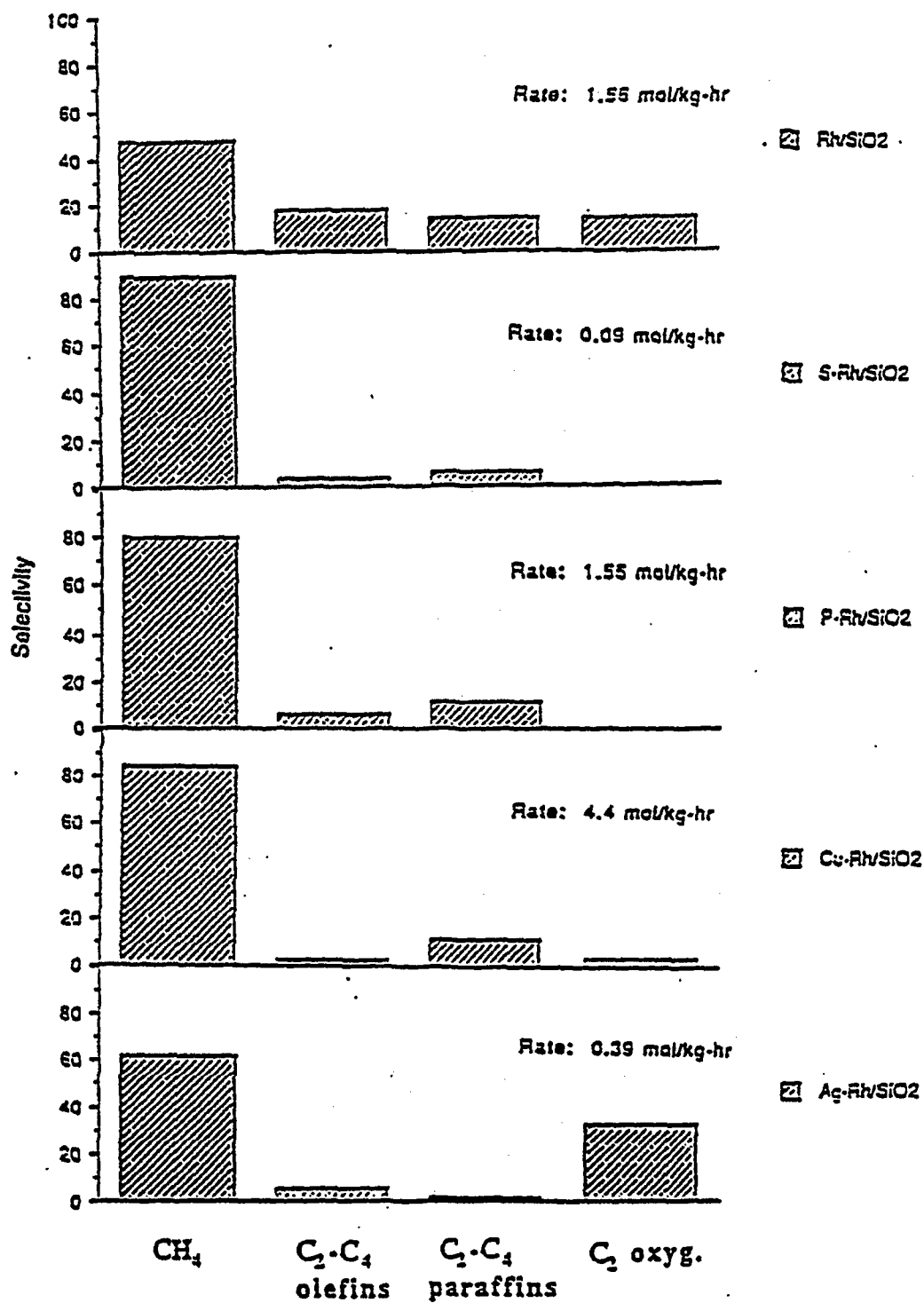


Figure 8.1 Selectivities of products from the reaction of CO/H_2 at 573 K and 10 atm

paraffins, and C_2 oxygenates (acetaldehyde and ethanol) were the main products. These selectivities are expressed in terms of the ratio of the rate of formation of that for a specific product to the total rate of product formation as shown in Figure 8.1.

The rate of CO conversion decreases in the order



The suppression of the overall CO hydrogenation brought about by P and S has also been reported for Ni catalysts [96,97,105]. The doping of P or S to Rh increase the selectivity of methane while decreasing the selectivity of olefins compared to the unpromoted catalyst. The Ag and S promoted catalysts show low paraffin selectivity while the others remained approximately the same. Rh catalysts modified with S or P exhibit no activity for C_2 oxygenates synthesis while Cu-Rh/SiO₂ shows a decrease and Ag-Rh/SiO₂ shows a more than doubled increase in the selectivity for C_2 oxygenates.

Previously, researchers have shown that C_2 oxygenates are formed by CO insertion to CH_x which is produced from CO dissociation followed by hydrogenation [20,22,39,59,60,82,164,165,167]. Figure 8.2 is the proposed reaction scheme. This mechanism shows that the formation of higher oxygenates and hydrocarbons go through a common CH_x intermediate. C_2 oxygenates, such as acetaldehyde and ethanol, are formed via the insertion of CO into adsorbed CH_x ; CH_4 is produced from hydrogenation of CH_x ; C_2 hydrocarbons are resulted from chain incorporation of CH_x . The variation in product distribution over these catalysts reflects the difference in catalytic activity for hydrogenation, CO insertion and chain growth.

Ethylene addition serves as an excellent probe reaction for the

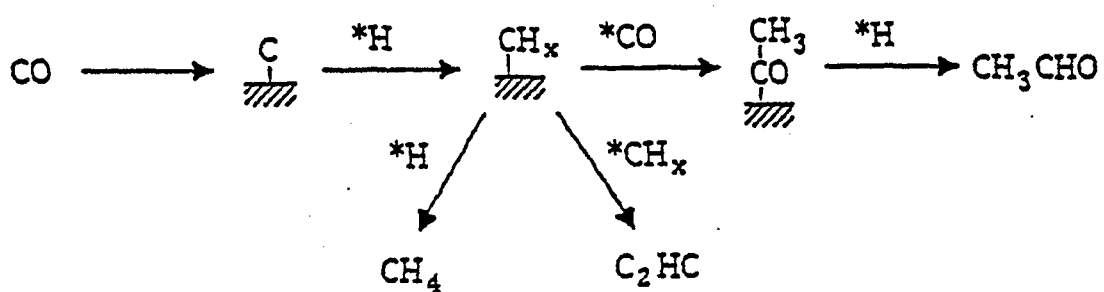


Figure 8.2 Reaction pathway for the CO hydrogenation reaction.

study of the effect of chemical addition on the specific reaction steps [39,57,82]. The selectivities for the products from ethylene addition are given in Figure 8.3. The mol% C_2H_4 in CO/H_2 , as shown in Figure 8.3, represents the mole fraction of ethylene added in the CO/H_2 reactant stream. Ethylene addition studies over Rh/SiO_2 have shown that increasing C_2H_4 concentration led to an increase in the rate of ethylene conversion but hardly affect the product selectivity [74]. The high rate of ethylene conversion on P- Rh/SiO_2 is due to the addition of a high concentration of ethylene. Thus, the selectivity is of a major concern here, which provides insight into the effect of additives on the specific reaction steps.

All of the catalysts produce no or a very little amount of methane and C_3 hydrocarbons indicating that the Rh-based catalysts are not active for catalyzing hydrogenolysis and chain growth. The major products in the ethylene addition reaction are ethane, propionaldehyde, and propanol. The catalysts modified with S, P, Cu, and Ag showed large increases in the ethane selectivity while decreases in the selectivity for propanol. The doping of additives Ag and S, however, increase the propionaldehyde selectivity while the addition of P and Cu to Rh/SiO_2 decrease with respect to the unpromoted catalyst.

Figure 8.4 shows the reaction scheme for the ethylene addition reaction [39,57,82]. The gaseous ethylene reacts with a surface hydrogen atom to form an adsorbed C_2H_5 intermediate. This intermediate can undergo CO insertion to form C_3 oxygenates (propionaldehyde and 1-propanol), hydrogenation to form ethane, or chain propagation to form C_4 hydrocarbons. High selectivity of the catalyst for C_3 oxygenates reflect the CO insertion activity of the catalyst. The higher

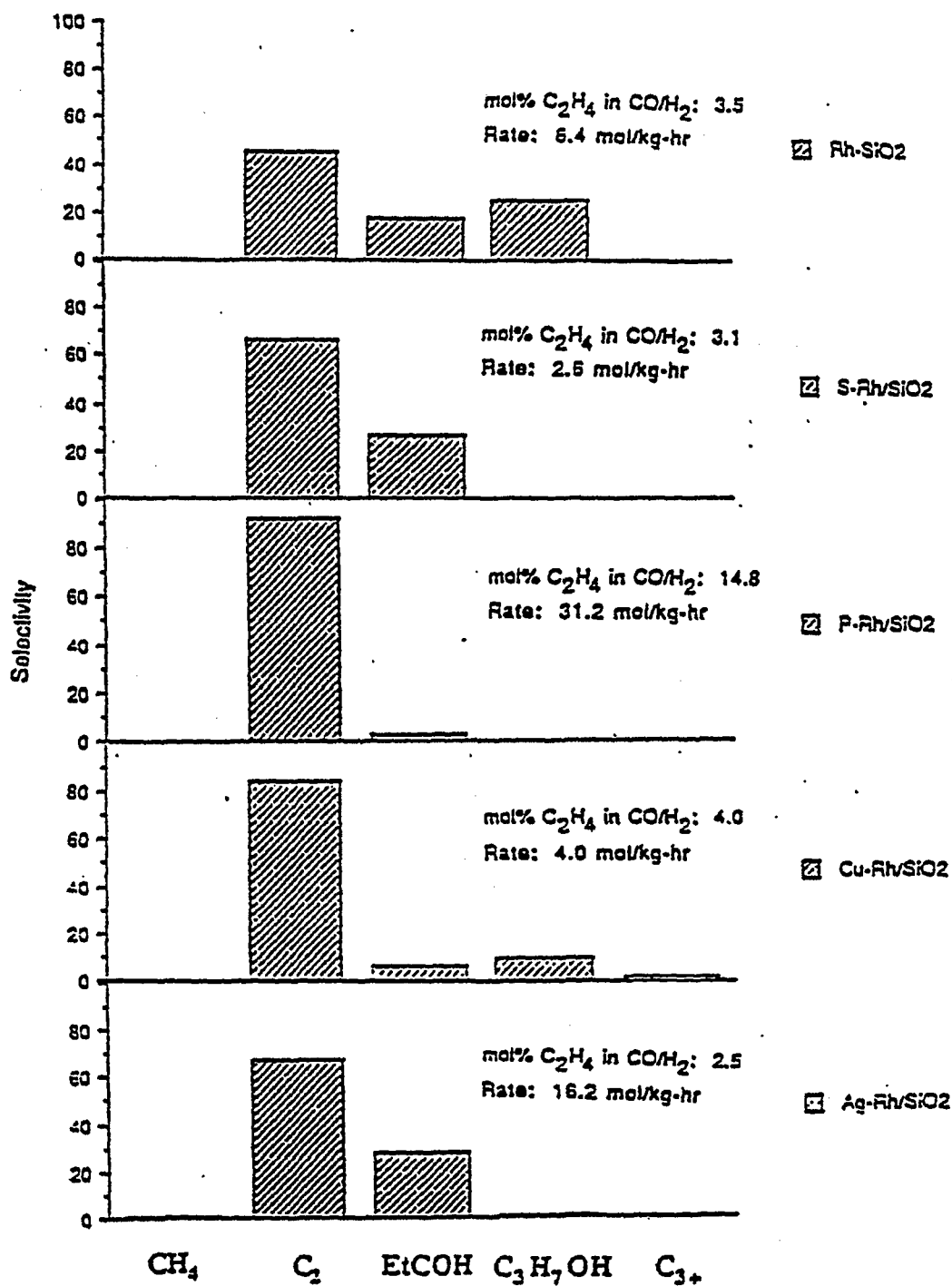


Figure 8.3 Selectivities of products from the reaction of CO/H₂/C₂H₄ at 573 K and 10 atm.

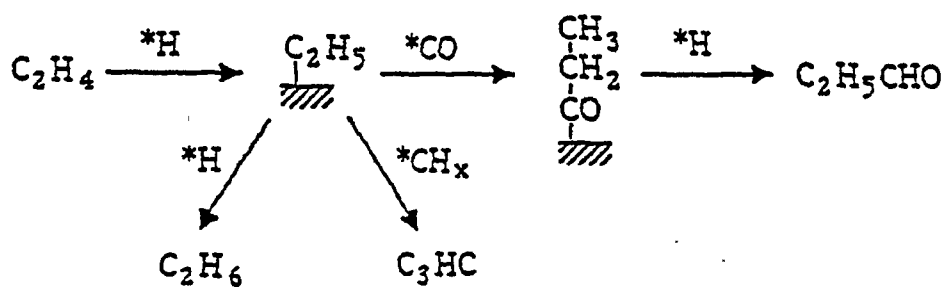


Figure 8.4 Reaction pathway for the ethylene addition reaction.

selectivity for propionaldehyde on S-Rh/SiO₂ and Ag-Rh/SiO₂ compared to Rh/SiO₂ suggest that S and Ag have a promotional affect on the CO insertion. Their low selectivity for propanol indicates their low activity for the hydrogenation of propionaldehyde to propanol. Additives, such as P and Cu appear to have a detrimental effect on the CO insertion as indicated by their low C₃ oxygenate selectivity.

A comparison of Figures 8.2 and 8.4 shows a very similar reaction scheme. The surface intermediates of CH_x in Figure 3 and C₂H₅ in Figure 4 both can undergo a common hydrogenation, chain propagation, or CO insertion step. The difference between the two is the precursor to these surface intermediates. The precursor to the CH_x intermediate is a surface carbon species produced by CO dissociation followed by hydrogenation. CO dissociation is an extra catalytic step for the formation of CH_x as compared to the C₂H₅ intermediate, which has gaseous ethylene as a precursor. Ethylene is a good probe molecule for the CO insertion step because there are no further complications from the CO dissociation step.

The additives P and Cu result in the higher methane formation in the CO hydrogenation reaction and higher ethane formation in the ethylene addition reaction. This indicates that P and Cu enhance the hydrogenation of the CH_x and C₂H₅ intermediates to hydrocarbons but suppress the CO insertion to C₂₊ oxygenates.

The addition of Ag results in an increase in C₂ oxygenate selectivity in CO hydrogenation and propionaldehyde selectivity in ethylene addition. This result indicates that Ag enhances the CO insertion reaction.

The S additive lowers the overall CO conversion rate in both

reactions by a substantial amount; however, in the ethylene addition reaction, more oxygenates were produced. The low CO conversion on S-Rh/SiO₂ is due to S poisoning the CO dissociation step [96,97].

Figure 8.5 summarizes the results of this study on the role of additives on the hydrogenation and CO insertion steps. The effects of other additives reported in the literature [57,79,82,158-160,162,166] are also included in the figure for comparison. Figure 8.5 provides a basis for the design of a more active and selective C₂ oxygenate synthesis catalyst. One possible way to fine tune catalyst activity and selectivity is by the use of multiple additives. Multiple additives can be used to enhance or suppress desired reaction steps. Further study on the effect of multiple addition is needed for the development of a practical multiple promoted catalyst.

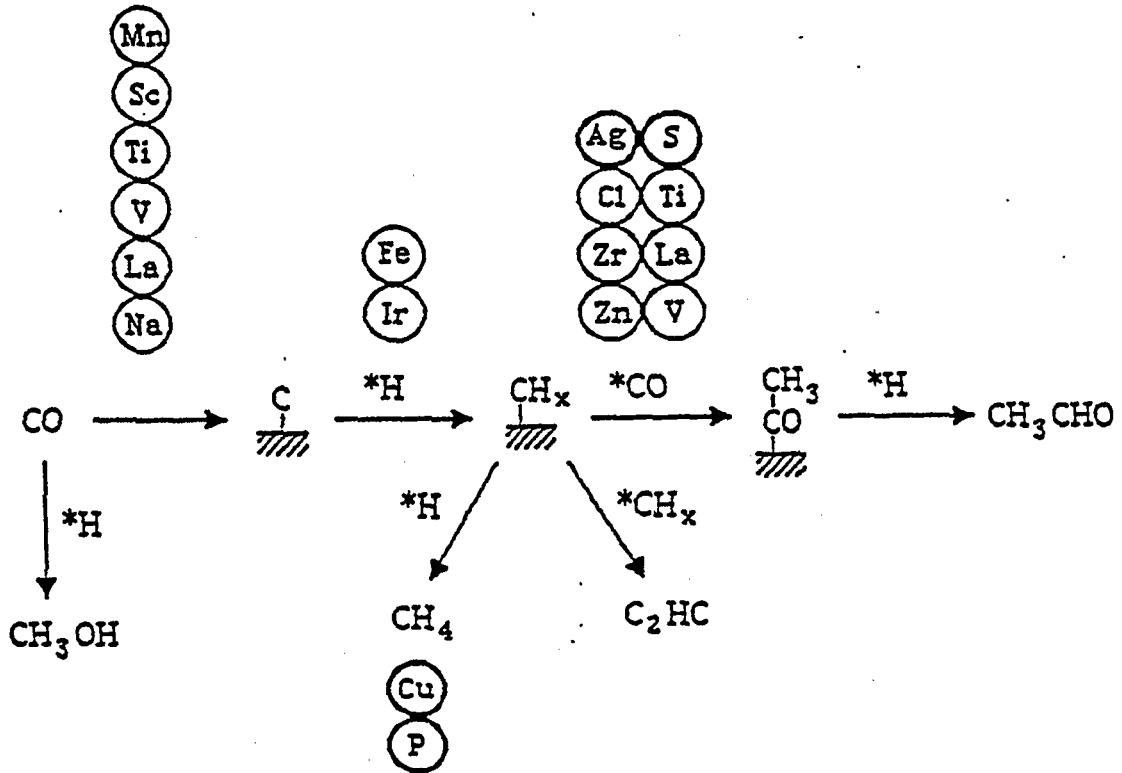


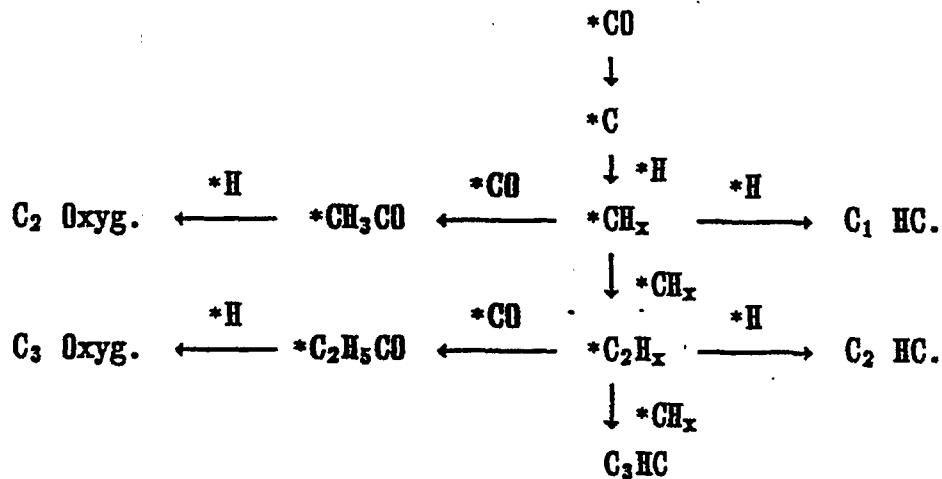
Figure 8.5 Reaction for the CO hydrogenation reaction with the additives that enhance specific steps.

CHAPTER IX

SUMMARY

9.1 Overview

This study is aimed at establishing the reaction mechanism of higher oxygenate synthesis from syngas and developing a better understanding of the effect of additives on the synthesis. Extensive studies in higher oxygenate synthesis have suggested that CO insertion is the key step for the formation of higher oxygenates such as acetaldehyde, ethanol, propionaldehyde, and propanol [36-44]. The reaction pathway for the formation of higher oxygenates from syngas is present in the following scheme.



*H: adsorbed hydrogen
 *CO: adsorbed CO
 *CH_x: adsorbed hydrocarbon
 *CH₃CO: adsorbed acyl

HC: hydrocarbon
 Oxyg: oxygenate

The nature of active site for the CO insertion step has been a controversial subject for more than a decade. Lack of understanding of the nature of active sites for the specific reaction step has greatly impeded the development of highly active and selective catalysts. 147

An in situ IR reaction system coupled with on-line GC has been developed to investigate the nature of the active site for CO insertion and the roles of additives in the higher oxygenate synthesis. Infrared spectra of CO adsorption on the catalyst surface have been employed to characterize the surface state of catalyst before, during, and after reaction. A molecular probing technique has been applied to investigate the reaction pathway for oxygenate synthesis and revealed the type of adsorbed CO involved in CO insertion and the effect of additives, such as silver and sulfur, on the synthesis.

9.2 CO Adsorption

Infrared spectra of CO adsorption on catalyst reveals the state of the catalyst surface. Infrared studies show that CO adsorption on the surface of Rh, Ru, and Ni produces linear CO, bridged CO, and carbonyl species [119-131]. The relative infrared intensity strongly depends on the geometric structure and electronic state of metal surfaces and conditions of reaction and adsorption [119,123-125]. Dicarbonyl has been shown to be formed on the highly dispersed metal surface where the metal atom possesses a positive charge [119-121,125]. Linear CO exhibiting an infrared band in the 2030-2070 cm^{-1} region and bridged CO are the dominant species on the surface of reduced metal crystallites. Figure 9.1 summarizes the infrared spectra of CO adsorption on reduced and sulfided catalysts at 513 K and 1 atm. CO adsorption on the reduced catalysts produces the following infrared

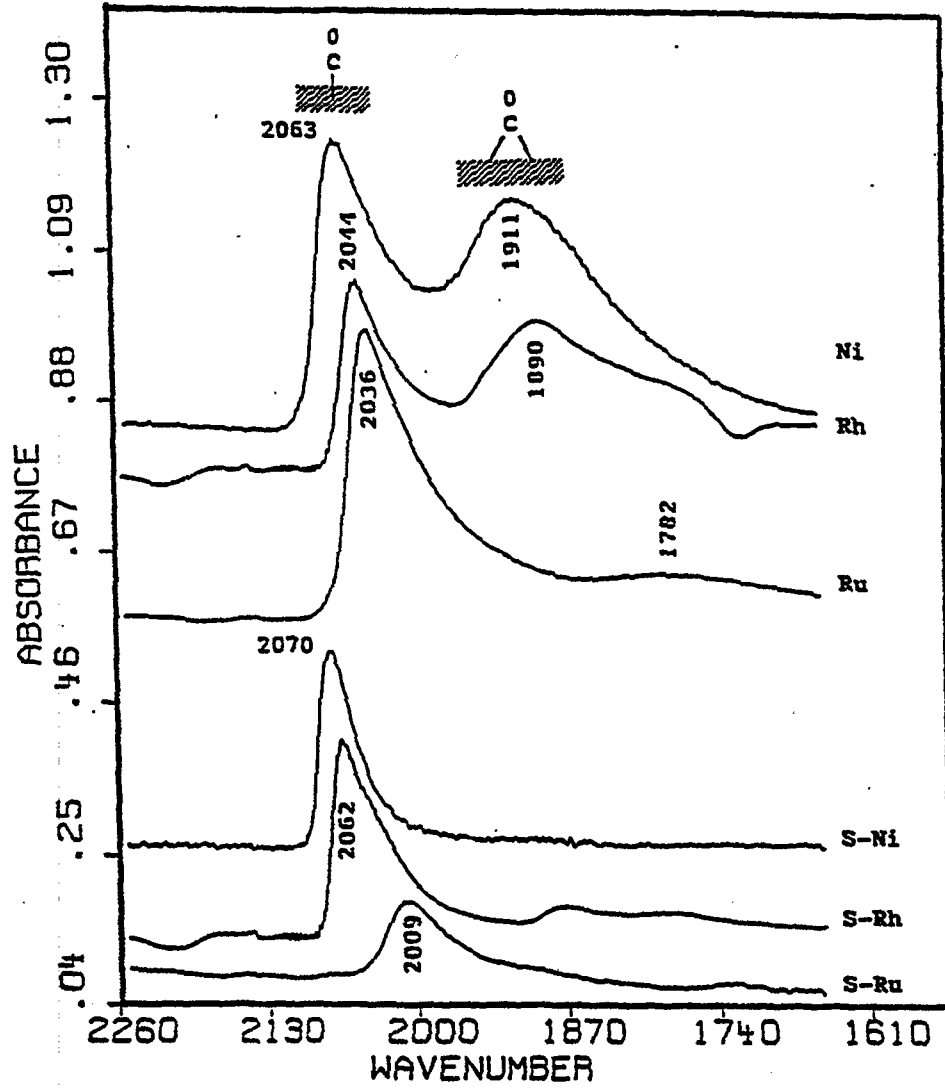


Figure 8.1 Infrared Spectra of CO Adsorption on Reduced and Sulfided Ni/SiO₂, Rh/SiO₂, and Ru/SiO₂ at 513 K, 1 atm.

spectra: linear CO at 2063 cm^{-1} and bridge CO at 1911 cm^{-1} for Ni/SiO₂; linear CO at 2044 cm^{-1} and bridge CO at 1890 cm^{-1} for Rh/SiO₂; linear CO at 2036 cm^{-1} and a broad bridge CO band near 1782 cm^{-1} for Ru/SiO₂. The observed wavenumbers of adsorbed CO are in good agreement with those reported for SiO₂-supported Ni, Rh, and Ru [119-131]. The presence of linear and bridge CO indicates that the surface of these reduced catalysts contain both single and pair-atom sites which are in zero valence state at 513 K.

The effect of adsorbed sulfur on the structure and state of the catalyst surface can be elucidated from infrared spectra of CO adsorption. Adsorbed sulfur appears to disrupt the adjacent pairs of metal atoms serving as bridge CO sites [98,112]. Therefore, the remaining surface metal may form isolated atoms which only permit adsorption of CO in the linear form. The variation of the linear CO intensity has been found to depend on the coverage of sulfur on the catalysts [112]. The adsorbed sulfur also alter adsorption characteristics of CO through metal-sulfur interactions. The upward shift of linear CO frequency can be attributed to the weakening of metal-CO bond as a result of metal-sulfur interactions. Such an effect has been observed on the sulfided Ni and Rh of which surface metals may possess partial positive charge [112,113]. In contrast, sulfidation of Ru led to a slightly downward shift of linear-CO wavenumber. The effect of adsorbed sulfur on CO adsorption on Ru has been shown to differ from those on Pt and Ni catalysts [97,108].

9.3 Nature of the Active Site for CO Insertion

Controversy on the active site for CO insertion has been primarily resulted from the lack of direct observation of active

species under reaction conditions. The in situ IR technique permits the investigation of active species on the catalyst surface under reaction conditions. In situ infrared studies of the reaction of C_2H_4/H_2 with adsorbed CO on reduced and oxidized Rh/SiO₂ catalysts reveals that the linear CO adsorbed on the single Rh⁰ site of the reduced Rh/SiO₂ and the linear CO adsorbed on the single Rh⁺ site of the oxidized Rh/SiO₂ are consumed and propionaldehyde is produced as adsorbed CO species react with C₂H₄ and H₂. The results show that both single Rh⁰ atoms and Rh⁺ ion sites are active for the CO insertion reaction. It can be concluded that the CO insertion step is more sensitive to the surface structure than to the electronic state of the surface.

The above conclusion has been further tested by ethylene hydroformylation on the oxidized and sulfided Rh/SiO₂. Oxidized Rh/SiO₂ containing considerable amounts of single Rh⁺ sites exhibits a higher rate and selectivity for the formation of propionaldehyde than the reduced Rh/SiO₂; the sulfided Rh/SiO₂ comprising mainly single Rh sites shows higher rate and selectivity for the formation of propionaldehyde than the reduced Rh/SiO₂. The low selectivity of the reduced Rh/SiO₂ for ethylene hydroformylation is attributed to the high hydrogenation activity of the Rh crystallite surface on the reduced Rh/SiO₂.

9.4 Effect of Silver on C₂ Oxygenate Synthesis

The XPS and CO and NO chemisorption data indicate that the presence of Ag tends to produce Rh⁺ ions and block the bridge CO sites on the surface of Rh particle. It is, therefore, expected that Ag should enhance the catalyst activity of CO insertion. Reaction studies

reveal that the selectivity and activity of Rh catalysts for C_2 oxygenate synthesis increased with Ag content. 151

9.5 Oxygenate Synthesis on Ni/SiO₂ and Ru/SiO₂ Catalysts

The high cost of Rh metal has prompted us to search for a potential substitute to the Rh metal. Ni and Ru were selected for this study because of low cost. The objective of the study is to elucidate the nature of CO insertion sites on these hydrocarbon synthesis catalysts and to shift the selectivity of the catalyst toward oxygenates.

The result of ethylene hydroformylation shows that Ni/SiO₂ exhibits CO insertion activity. Linear CO and bridge CO were observed at conditions of 513 K and 10-30 atm. Sulfidation of Ni/SiO₂ leads to a blockage of bridge CO sites, an inhibition of ethylene hydrogenation, and an enhancement of the formation of propionaldehyde from ethylene hydroformylation. The result further confirms that isolated atom sites are responsible for CO insertion leading to the formation of propionaldehyde in ethylene hydroformylation. However, Ni catalyst tends to react with CO resulting in the formation of toxic Ni(CO)₄. Suppression of the formation of Ni(CO)₄ under reaction conditions is required.

On Ru/SiO₂ catalyst, the dominant CO species at CO adsorption, CO hydrogenation, and ethylene hydroformylation is linear CO. CO insertion was observed in CO hydrogenation reaction and in ethylene hydroformylation. Sulfidation of the Ru/SiO₂ catalyst severely suppressed CO hydrogenation reactivity. Both fresh and sulfided Ru/SiO₂ catalysts exhibit hydroformylation activity. However, the presence of sulfur reduces the rate of propionaldehyde formation. The

transient and temperature-programmed reaction studies revealed that 152
sulfur poisoning of Ru/SiO₂ catalyst for ethylene hydroformylation was
due primarily to the inhibition of desorption of propionaldehyde from
the sulfided Ru/SiO₂.

9.6 Effect of Additives

The following can be concluded from the study on the effects of
various additives for the production of higher oxygenates over Rh/SiO₂
catalysts:

- (1) Addition of S suppresses the CO dissociation step and
enhances the CO insertion step, therefore lowering the
overall product rate but increasing the oxygenate
selectivity in ethylene addition.
- (2) Addition of P or Cu enhance the CH_x intermediate
hydrogenation, therefore increasing the methane formation.
- (3) Addition of Ag enhances the CO insertion activity,
therefore increasing the C₂₊ oxygenate selectivity.

9.7 Concluding Remarks

The study identifies that both single Rh⁰ atom and Rh⁺ ion
sites are active for the CO insertion reaction. Linear CO on the Rh⁺
site appears to be more active for CO insertion than that on the
reduced Rh⁰ site. Synthesis of C₂₊ oxygenates requires both the active
sites for CO insertion and the ensemble of Rh metal atoms for the
formation of alkyl species. Thus, the activity and selectivity of
catalyst for C₂₊ oxygenate synthesis lies in the concentration of Rh⁺
sites, single Rh⁰ sites, and Rh ensemble sites. Enhancement of C₂₊
oxygenate synthesis activity by the use of Ag promoter suggests that
highly selective and active catalysts for the synthesis can be prepared

by the careful construction of specific active sites using various types of promoters.

BIBLIOGRAPHY

1. Eukland, E.E., and Mills, G.A., ChemTech. 549 (1989).
2. Matare, H.F., "Energy: Facts and Future," CPC Press. Inc., Florida, 1989.
3. Probststein, R.F., and Hicks, R.E., "Synthetic Fuels," McGraw Hill, New York, 1982.
4. Haggin, J., C&EN. May 19. p. 7. 1986.
5. Courty, P., Durand, D., Freund, E., and Sugier, A., J. Mol. Catal. 17, 241 (1982).
6. Fan, W.X., Gao, R., and Griffith, G.L., J. Catal. 114, 447 (1988).
7. Nunan, J.G., Bogdan, C.E., Klier, K., Smith, K.J., Young, C.W., and Herman, R.G., J. Catal. 116, 195 (1989).
8. Anderson, R.B., "Fisher Tropsch and Related Syntheses," Academic Press, New York, 1983.
9. Bhasin, M.M., and O'Conor, G.L., Belgian Patent, 824,822 (1975).
10. Ichikawa, M., Bull. Chem. Soc. Jpn. 51, 2273 (1978).
11. Sachtler, W.M.H., in "Proceedings, International Congress on Catalysis, 8th," vol. 1, p. 151. 1984.
12. Yoneda, Y., "Progress in C₁ Chemistry in Japan," Elsevier, 1989.
13. Peri, J.B., in "Catalysis, Science and Technology," (J.R. Anderson and M. Boudart Eds.), vol. 5, p. 172. Springer-Verlag, New York, 1984.
14. Arakawa, H, Fukushima, T., and Ichikawa, M., Appl. Spec. 40, 884 (1986).
15. Bradshaw, A.M., Hoffman, F.M., Surf. Sci. 72, 513 (1978).
16. Solymosi, F., and Pasztor, M., J. Phys. Chem, 89, 4789 (1985).
17. Li, Y.E., and Gonzalez, R.D., J. Phys. Chem. 92, 1589 (1988).

18. Vannices, M.A., *Cat. Rev. Sci. Eng.* 14, 153 (1976).
19. Ponec, V., *Cat. Rev. Sci. Eng.* 18, 151 (1978).
20. Biloen, P., and Sachtler, W.M.H., in "Advances in Catalysis," (D.D. Eley, H. Pines, and P.B. Weisz, Eds.), Vol. 30, p.165. Academic Press, New York, 1981.
21. Somorjai, G.A., *Cat. Rev. Sci. Eng.* 23, 189 (1981).
22. Bell, A.T., *Cat. Rev. Sci. Eng.* 23, 203 (1981).
23. Ekerdt, J.G., and Bell, A.T., *J. Catal.* 58, 170 (1979).
24. Cant, N.W., and Bell, A.T., *J. Catal.* 73, 257 (1982).
25. Erdoheleyi, A., and Solymosi, F., *J. Catal.* 84, 446 (1983).
26. Biloen, P., Helle, N.J., van den Berg, F.G.A., and Sachtler, W.M.H., *J. Catal.* 81, 450 (1983).
27. Happel, J., Cheh, H.Y., Otarod, M., Ozawa, S., Severdia, A.J., Yoshida, T., and Fthenakis, V., *J. Catal.* 75, 314 (1982).
28. Reymond, J.P., Meriaudeau, P., Pommier, B., and Bennett, C.O., *J. Catal.* 64, 163 (1980).
29. Stockwell, D.M., Chung, J.S., and Bennett, C.O., *J. Catal.* 112, 135 (1988).
30. Ichikawa, M., Fukushima, T., and Shikakura, K., in "Proceedings, International Congress on Catalysis, 8th," vol. 2, p. 69. 1984.
31. Winslow, P., and Bell, A.T., *J. Catal.* 85, 158 (1984).
32. Stockwell, D.M., Bianchi, D., and Bennett, C.O., *J. Catal.* 113, 13 (1988).
33. Stockwell, D.M., and Bennett, C.O., *J. Catal.* 110, 354 (1988).
34. Kellner, C.S., and Bell, A.T., *J. Catal.* 70, 418 (1981).
35. Kobori, Y., Yamasaki, H., Naito, S., Onishi, T., and Tamaru, K., *J. Chem. Soc. Faraday Trans. I*, 78, 1473 (1982).
36. Orita, H., Naito, S., and Tamaru, K., *J. Catal.* 90, 183 (1984).
37. Henrici-Olive, G., and Olive, S., *J. Mol. Catal.* 24, 7 (1984).
38. Underwood, R.P., and Bell, A.T., *J. Catal.* 111, 325 (1988).
39. Sachtler, W.M.H., and Ichikawa, M., *J. Phys. Chem.* 90, 4752 (1986).

40. van den Berg, F.G.A., Glezer, J.H.E., and Sachtler, W.M.H., J. Catal. 93, 340 (1985). 157
41. Satchler, W.M.H., Shriver, D.F., Hollenberg, W.B., and Lang, A.F., J. Catal. 93, 429 (1985).
42. Satchler, W.M.H., Shriver, D.F., Ichikawa, M., J. Catal. 99, 513 (1985).
43. Ichikawa, M., and Fukushima, T., J. Chem. Soc. Chem. Commun. 321 (1985).
44. van der Lee, G., and Ponec, V., J. Catal. 99, 511 (1986).
45. Evans, D., Osborn, J.A., and Wilkinson, G., Inorg. Phys. Theor. 3133 (1968).
46. Calderazzo, F., Angew. Chem. Int. Ed. Engl. 16, 299 (1977).
47. Parshall, G. W., "Homogeneous Catalysis - The Applications and Chemistry of Catalysis by Soluble Transition Metal Complexes," p. 85. Wiley, New York, 1981.
48. Pino, P., Piacenti, F., and Bianchi, M., in "Organic Synthesis via Metal Carbonyls," (I. Wender, and P. Pino, Eds.). Vol. 2, p. 43. Wiley, New York, 1977.
49. Masters, C., "Homogeneous Transition-Metal Catalysis - a General Art," p. 102. Chapman and Hall, New York, 1891.
50. Noack, K., and Calderazzo, F., J. Organometal. Chem. 10, 101 (1967).
51. Keim, W., "Catalysis of C₁ Chemistry," D. Redel, Netherlands, 1983.
52. Cornils, B., in "New Synthesis with Carbon Monoxide," (J. Falbe, Ed.), p. 1. Springer-Verlag, Berlin, 1988.
53. Paulik, F.E., Cat. Rev. Sci. Eng. 6, 49 (1972).
54. Naito, S., and Tanimoto, M., J. Catal. 130, 106 (1991).
55. Chuang, S.S.C., and Pien, S.I., J. Mol. Catal. 55, 12 (1989).
56. Cotton, F.A., and Wilkinson, G., "Advanced Organic Chemistry," p. 1233. Wiley, 1988.
57. Chuang, S.C., Tian, Y.H., Goodwin, J.G. Jr., and Wender, I., J. Catal. 96, 396 (1985).
58. Watson, P.R., and Somorjai, G.A., J. Catal. 72, 347 (1981).

59. Watson, P.R., and Somorjai, G.A., *J. Catal.* 74, 282 (1982).
60. Ichikawa, M., *Chemtech.* 674 (1982).
61. Kellner, C.S., and Bell, A.T., *J. Catal.* 71, 288 (1981),
62. Kuijpers, E.G.M., Kock, A.J.H.M., Nieuwesteeg, M.W.C.M., and Geus, J.W., *J. Catal.* 95, 13 (1985).
63. Stockwell, D.M., Chung, J.S., and Bennett, C.O., *J. Catal.* 112, 135 (1988).
64. Wilson, T.P., Kasai, P.H., and Ellgen, P.C., *J. Catal.* 69, 193 (1981).
65. Kawai, M., Uda, M., and Ichikawa, M., *J. Phys. Chem.* 89, 1654 (1985).
66. van der Lee, G., Schuller, B., Post, T., Favre, T.L.F., and Ponec, V., *J. Catal.* 98, 522 (1986).
67. Katzer, J.R., Sleight, A.W., Gajarsdo, P., Mjichel, J.B., Gleason, E. F., and McMillian, S., *Faraday Diss. Chem. Soc.* 72, 121 (1981).
68. Gysling, H. J., Monnier, J.R., and Apai, G., *J. Catal.* 103, 407 (1987).
69. Ford, R.R., in "Advances in Catalysis," (D.D. Eley, H. Pines, and P.B. Weisz Eds.), vol. 21, p. 51. Academic Press, New York, 1970.
70. Vannice, M.A., *J. Catal.* 37, 462 (1975).
71. Storch, H.H., in "Advances in Catalysis," (W.G. Frankzenburgh, and E.K. Rideal, Eds.), vol. 1, p. 115. Academic Press, New York, 1948.
72. Vannice, M.A., *J. Catal.* 50, 228 (1977).
73. Favre, T. L. F., van der Lee, G., Ponec, V., *J. Chem. Soc. Che. Commun.* 230 (1985).
74. Sze, C., "The effect of Sulfur on the Oxygenate Synthesis over Silica Supported Rh, Ru, and Ni ." M.S. Thesis, Univ. of Akron, 1988.
75. Trimm, D. L., "Design of Industrial Catalysts," Elsevier, Amsterdam, 1980.
76. Bond, G. C., in "Metal-Support and Metal-Additive Effects in Catalysis" (B. Imelik et al., Eds.) Elsevier, Amsterdam, 1982.
77. Ichikawa, M., *Bull. Chem. Soc. Jpn.* 51, 2268 (1978).

78. Ichikawa, M., Sekizawa, K., Shikakura, K., J. Mol. Catal. 11, 167 (1982). 159
79. Kagami, S., Naito, O., Kikuzono, S., and Tamaru, K., J. Chem. Soc. Commun. 256 (1983).
80. Enomoto, T., Kata, K., Okuhara, T., and Misono, M., Bull. Chem. Soc, Jpn. 60, 1237 (1987).
81. Chuang, S.C., Goodwin, J.G., Jr., Wender, I., J. Catal. 92, 416 (1985).
82. Chuang, S.C., Goodwin, J.G., Jr., Wender, I., J. Catal. 95, 435 (1985).
83. Ichikawa, M., Lang, A.J., Shriver, D.F., and Sachtler, W.M.H., J. Am. Chem. Soc. 107, 7216 (1985).
84. Jen, H.W., Zheng, Y., Shriver, D.F., and Sachtler, W.N.H., J. Catal. 116, 361 (1989).
85. Soma-Noto, Y., Sachtler, W.M.H., J. Catal. 32, 312 (1974).
86. Premit, M., Matthieu, M., and Sachtler, W.M.H., J. Catal. 44, 324 (1976).
87. Campbell, C.T., and Goodman, D.W., Surf. Sci., 123, 423 (1982).
88. Mori, Y., Mori, T., Hattori, T., and Murakami, Y., J. Phys. Chem. 94, 4575 (1990).
89. Orita, H., Naito, S., and Tamaru, K., J. Phys. Chem. 89, 3066 (1985).
90. Haller, G.L., and Resasco, D.E., in "Advances in Catalysis." (D.D. Eley, H. Pines, and P.B. Weisz, Eds.), vol. 36, p. 173. Academic Press, New York, 1989.
91. Fukuoka, A., Ichikawa, M., Hriljac, J.A., and Shriver, D.F., Inorg. Chem. 26, 3645 (1987).
92. Stevenson, S.A., Lisitsyn, A., and Knozinger, H., J. Phys. Chem. 94, 1576 (1990).
93. Fukushima, T., Arakawa, H., and Ichikawa, M., J. Chem. Soc. Chem. Commun. 729 (1985).
94. Tatsumi, T., Muramatsu, A., Yokota, K., Tominaga, H., J. Catal. 115, 388 (1989).
95. Jordan, D. S., and Bell, A. T., J. Phys. Chem. 90, 4797 (1986).

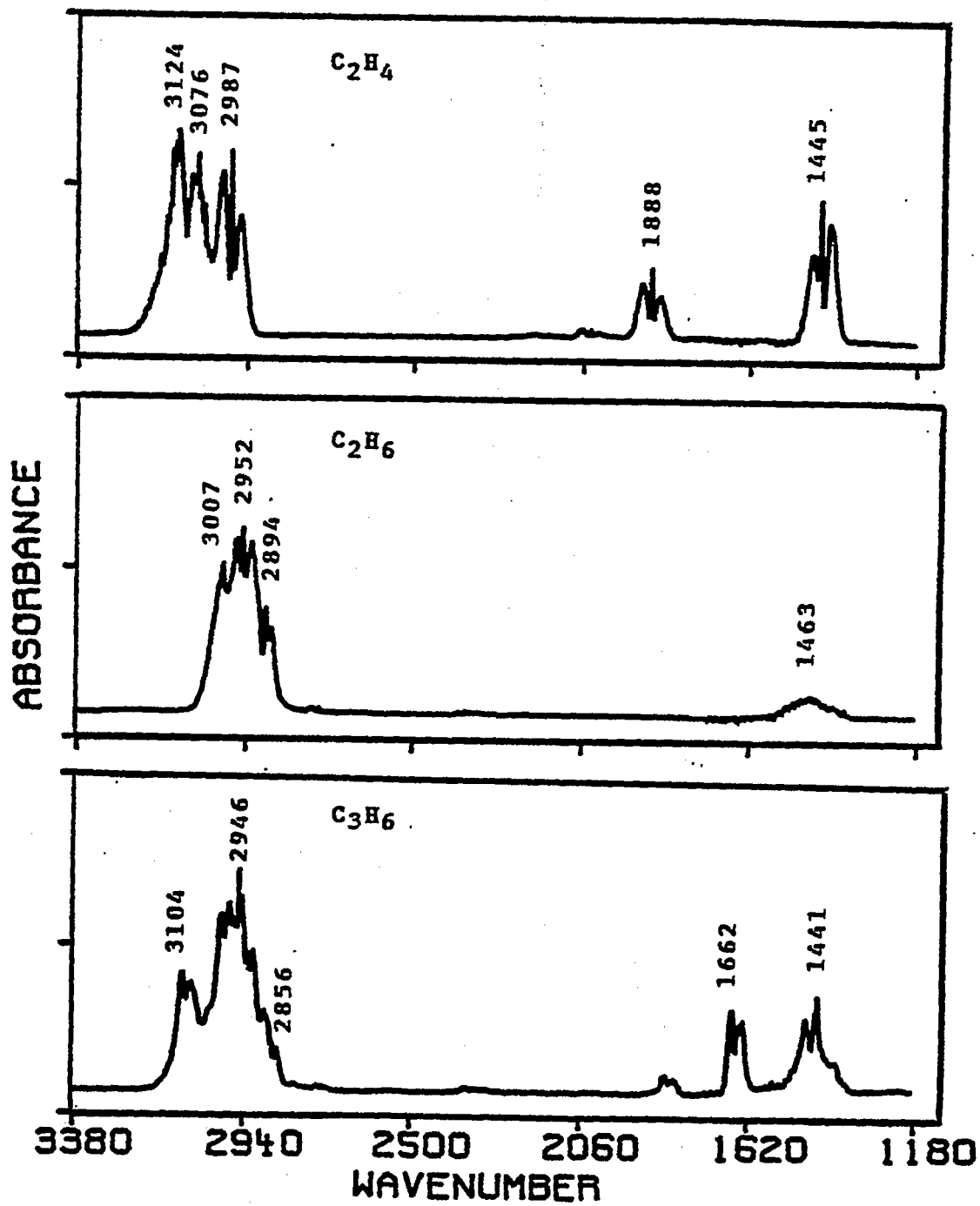
96. Bartholomew, C.H., Agrawal, P.K., and Katzer, J.R., in "Advances in Catalysis" (D. D. Eley, H. Pines, and P. B. Weisz, Eds.), Vol. 30, p. 135. Academic Press, New York, 1982.
97. Oudar, J., in "Deactivation and Poisoning of Catalysts" (J. Oudar and H. Wise, Eds.), p. 51. Dekker, New York, 1985.
98. Goodman, D.W., in "Heterogeneous Catalysis," (B.L. Shapiro, Ed.), vol.2, p. 230. A&M Univ. Press, Texas, 1984.
99. Delescluse, P., and Masson, A., Surf. Sci. 100, 423 (1980).
100. Fischer, G.B., Surf. Sci. 87, 215 (1979).
101. Ng, C.F., and Martin, G.A., J. Catal. 54, 384 (1978).
102. Pannell, R.B., Chung, K.S., and Bartholomew, C.H., J. Catal. 46, 340 (1977).
103. Oliphant, J.L., Fowler, R.W., Pannell, R.B., and Bartholomew, C.H., J. Catal. 51, 229 (1978).
104. Rendulic, K.D., and Winkler, A., Surf. Sci. 74, 318 (1978).
105. Kiskinova, M., and Goodman, W.D., Surf. Sci. 108, 64 (1981).
106. Johnson, S., and Madix, R.J., Surf. Sci. 108, 77 (1981).
107. Schwarz, J.A., Surf. Sci. 87, 525 (1979).
108. Schwarz, J.A., and Kelemen, S.R., Surf. Sci. 87, 510 (1979).
109. Neff, L.D., and Kitching, S.C., J. Phys. Chem. 78, 1648 (1974).
110. Bartholomew, C.H., and Pannell, R.B., Appl. Catal. 2, 39 (1982).
111. Jackson, S.D., Brandreth, B.J., and Winstanley, D., J. Chem. Soc. Faraday Tran. I, 83, 1835 (1987).
112. Konishi, Y., Ichikawa, M., and Sachtler, W.M.H., J. Phys. Chem. 91, 6286 (1987).
113. Guerra, C.R., J. Colloid. Interface Sci. vol. 29, No. 2, p. 229. 1969.
114. Chuang, S.S.C., Pien, S.I., and Sze, C., J. Catal. 126, 187 (1990).
115. Colthup, N.B., Daly, L.H., and Wiberley, S.E., "Introduction to Infrared and Raman Spectroscopy," Academic Press, New York, 1964.
116. Greenler, R.G., Snider, D.R., Witt, D., and Sorbello, R.S., Surf. Sci. 118, 415 (1982).

117. Hair, M. L., "Infrared Spectroscopy in Surface Chemistry," Marcel Dekker Inc., New York, 1967.
118. Stoop, F., Toolenar, F.J.C.M., and Ponec, V. J. Catal. 73, 50 (1982).
119. Yang, A.C., and Garland, C.W., J. Phys. Chem. 61, 1504 (1957).
120. Yates, J.T., Jr., Duncan, T.M., Worley, S.D., and Vaughn, R.W., J. Chem. Phys. 70, 1219 (1979).
121. Cavanagh, R.R., and Yates, J.T., Jr., J. Chem. Phys. 74, 4150 (1981).
122. Solymosi, F., Tombacz, I., and Docsis, M., J. Catal. 75, 78 (1982).
123. Rice, C.A., Worley, S.D., Curtis, C.W., Guin, J.A., and Tarrer, A.R., J. Chem. Phys. 74, 6487 (1981).
124. Worley, S.D., Rice, C.A., Mattson, G.A., Curtis, C.W., Guin, J.A., and Tarrer, A.R., J. Chem. Phys. 76, 20 (1982).
125. Worley, S.D., Rice, C.A., Mattson, G.A., Curtis, C.W., Guin, J.A., and Tarrer, A.R., J. Phys. Chem. 86, 2714 (1982).
126. Dictor, R., and Roberts, S., J. Phys. Chem. 93, 2526 (1989).
127. Dalla Betta, R.A., and Shelef, M., J. Catal. 48, 111 (1977).
128. Yokomizo, G.H., Louis, C., and Bell, A.T., J. Catal. 120, 1 (1989).
129. Primet, M., Dalmon, J.A., and Martin, G.A., J. Catal. 46, 25 (1977).
130. Blackmond, D.G., and Ko, E.I., J. Catal. 96, 210 (1985).
131. Peri, J.B., Discuss. Faraday Soc. 41, 121 (1966).
132. Okuhara, T., Kimura, T., and Misono, Bull. Chem. Soc. Jpn. 57, 938 (1984).
133. Solymosi, F., Tombacz, I., and Kocsis, M., J. Catal. 75, 78 (1982).
134. Beebe, T. P., and Yates, J. T., Jr., J. Phys. Chem. 91, 254 (1987).
135. Soma, Y., J. Catal. 59, 239 (1979).
136. Fukushima, T., Arakawa, H., and Ichikawa, M., J. Phys. Chem. 89, 4440 (1985).

137. King, D.L., *J. Catal.* 61, 77 (1980).
138. Primet, M., and Sheppard, N., *J. Catal.* 41, 258 (1976).
139. Lucchesi, P.J., Carter, J.L., and Yates, D.J.C., *J. Phys. Chem.* 66, 1451 (1962).
140. Blyholder, G., Shihabi, D., Wyatt, W.V., and Bartlett, R., *J. Catal.* 43, 122 (1976).
141. Cross, R.J., in "Catalysis," (G.C. Bond, and G. Webb, Eds.), vol. 5, p. 366. The Royal Society of Chemistry, London, 1982.
142. Butts, S.B., Strauss, S.H., Holt, E.M., Syimson, R.E., Alcock, N.E., and Shriver, D.E., *J. Am. Chem. Soc.* 102, 5093 (1980).
143. Pichler, H., Schulz, H., and Elstner, M., *Brennst. Chem.* 48, 78 (1967).
144. Solymosi, F., and Pasztor, M., *J. Phys. Chem.* 89, 4789 (1985).
145. Basu, P., Panayotov, D., and Yates, J.T., Jr., *J. Phys. Chem.* 91, 3113 (1987).
146. Basu, P., Panayotov, D., and Yates, J.T., Jr., *J. Am. Chem. Soc.* 110, 2074 (1988).
147. Lu, K., and Tatarchuk, B.J., *J. Catal.* 106, 166 (1987).
148. Miura, H., Hondou, H., Sugiyama, K., Mastuda, T., and Gonzalez, R.D., in "Proceedings, International Congress on Catalysis, 9th," p. 1370. 1988.
149. Narita, T., Miyra, H., Sugiyama, K., Mastuda, T., and Gongalez, R.D., *J. Catal.* 103, 492 (1987).
150. Lyagba, E.T., Hoost, T.E., Nwalor, J.U., and Goodwin J.G., Jr., *J. Catal.* 123,1 (1990).
151. van Slooten, R.F., and Nieuwenhuys, B.E., *J. Catal.* 122, 429 (1990).
152. Hecker, W.C., and Bell, A.T., *J. Catal.* 49, 345 (1977).
153. Arai, H., and Yominaga, H., *J. Catal.* 43, 131 (1976).
154. Solymosi, F., Bansagi, T., and Novak, E., *J. Catal.* 112, 183 (1988).
155. Navak, E., and Solymosi, F., *J. Catal.* 125, 112 (1990).
156. Brown, M.F., and Gonzalez, R.D., *J. Catal.* 44, 477 (1976).

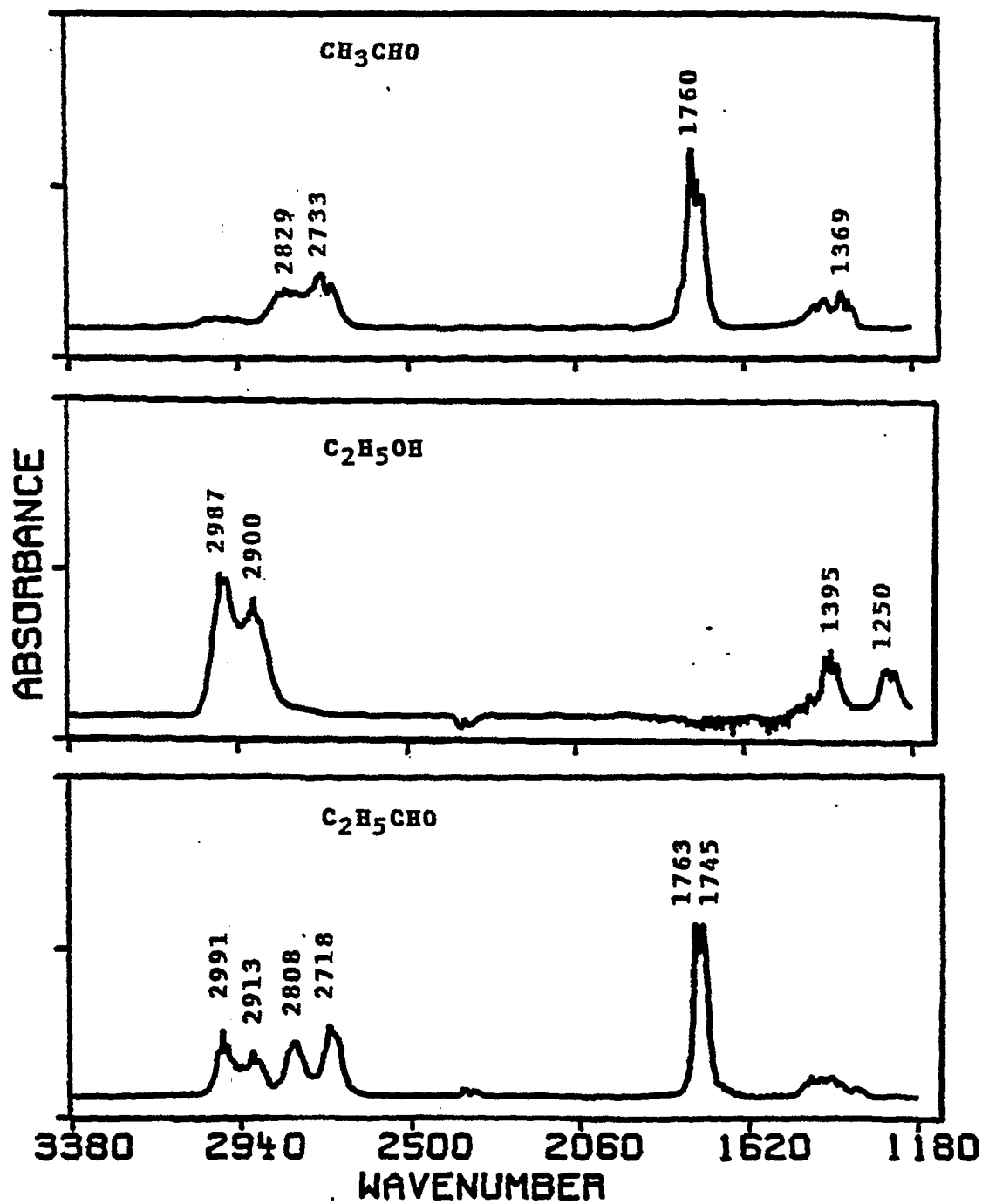
157. Chuang, S.S.C., Pien, S.I., and Narayanan, R., Appl. Catal. 57, 241 (1990).
158. Arakawa, H., Hanaoka, T., Takeuchi, K., Matsuzaki, T., Sugi, Y., in "Proceedings, International Congress on Catalysis, 9th", vol. 2, p. 602 1988.
159. Bastein, A.G.T.M., van der Boogert, W.J., van der Lee, G., Lico, H., Schuller, Ponec, V., Appl. Catal., 29, 243, (1987).
160. Benedetti, A., Carimati, A., Marengo, S., Martinengo, S., Pinna, F., Tessari, R., Strukul, G., Zerlia, T., Zanderighi, L., J. Catal., 122, 330 (1990).
161. Kienneman, A., Diagne, C., Hindermann, J.P., Chaumette, P., Courty, P., Appl. Catal., 53, 197 (1989).
162. Kip, B.J., Hermans, E.G.F., Prins, R., Appl. Catal., 35, 289 (1987).
163. Murchison, C.B., Conway, M.M., Stevens, R.R., Quarderer, G.J., in "Proceedings, International Congress on Catalysis, 9th", vol. 2, p. 662 1988.
164. Orita, H., Naito, S., Tamaru, K., Chem. Lett., 1161 (1983).
165. Cross, R.J., in "Catalysis," (G.C. Bond, and G. Webb, Eds.), vol. 5, p. 366. The Royal Society of Chemistry, London, 1982.
166. Underwood, R.P., Bell, A.T., Appl. Catal., 34, 289, (1987).
167. van der Berg, F.G.A., Ph.D., Dissertation, University of Leiden, The Netherlands (1984).

APPENDIX A
INFRARED SPECTRA OF GASEOUS HYDROCARBONS



APPENDIX B

INFRARED SPECTRA OF GASEOUS ALCOHOLS AND ALDEHYDES



SATISFACTION GUARANTEED

NTIS strives to provide quality products, reliable service, and fast delivery. Please contact us for a replacement within 30 days if the item you receive is defective or if we have made an error in filling your order.

▲ **E-mail: info@ntis.gov**

▲ **Phone: 1-888-584-8332 or (703)605-6050**

Reproduced by NTIS

National Technical Information Service
Springfield, VA 22161

This report was printed specifically for your order from nearly 3 million titles available in our collection.

For economy and efficiency, NTIS does not maintain stock of its vast collection of technical reports. Rather, most documents are custom reproduced for each order. Documents that are not in electronic format are reproduced from master archival copies and are the best possible reproductions available.

Occasionally, older master materials may reproduce portions of documents that are not fully legible. If you have questions concerning this document or any order you have placed with NTIS, please call our Customer Service Department at (703) 605-6050.

About NTIS

NTIS collects scientific, technical, engineering, and related business information – then organizes, maintains, and disseminates that information in a variety of formats – including electronic download, online access, CD-ROM, magnetic tape, diskette, multimedia, microfiche and paper.

The NTIS collection of nearly 3 million titles includes reports describing research conducted or sponsored by federal agencies and their contractors; statistical and business information; U.S. military publications; multimedia training products; computer software and electronic databases developed by federal agencies; and technical reports prepared by research organizations worldwide.

For more information about NTIS, visit our Web site at <http://www.ntis.gov>.

NTIS

**Ensuring Permanent, Easy Access to
U.S. Government Information Assets**



U.S. DEPARTMENT OF COMMERCE
Technology Administration
National Technical Information Service
Springfield, VA 22161 (703) 605-6000
